

Structural health monitoring of innovative civil engineering structures in Mainland China

Hong-Nan Li^a, Dong-Sheng Li^{*}, Liang Ren^b, Ting-Hua Yi^c, Zi-Guang Jia^d and Kun-Peng Li^e

State Key Lab of Coastal and Offshore Engineering, Faculty of Infrastructure Engineering, Dalian University of Technology, Dalian 116023, P.R. China

(Received December 20, 2015, Revised February 18, 2016, Accepted March 1, 2016)

Abstract. This paper describes the backgrounds, motivations and recent history of structural health monitoring (SHM) developments to various types of engineering structures. Extensive applications of SHM technologies in bridges, high-rise buildings, sport avenues, offshore platforms, underground structures, dams, etc. in mainland China are summarily categorized and listed in tables. Sensors used in implementations, their deployment, damage identification strategies if applicable, preliminary monitoring achievements and experience are presented in the lists. Finally, existing problems and promising research efforts in civil SHM are discussed, highlighting challenges and future trends.

Keywords: structural health monitoring; large-span civil infrastructure; high-rise buildings; damage identification; data normalization

1. Introduction

In China, more and more newly built large infrastructures, buildings, pedestrian and vehicular bridges, large sport avenues, offshore petroleum platforms, tunnels, heritage structures, port facilities and geotechnical structures, are equipped with recently emerged SHM systems because unpredicted structural failure may cause economic, catastrophic, and human life loss. An effective and reliable monitoring system is crucial to maintain safety and integrity of structures (Yi and Li 2012). The SHM usually refers to “the use of in-situ, continuous or regular (routine) measurement and analyses of key structural and environmental parameters under operating conditions, for the purpose of warning impending abnormal states or accidents at an early stage to avoid casualties as well as giving maintenance and rehabilitation advices” (Li *et al.* 2004). These structures are then expected to switch from the limited and intermittent manual inspection or maintenance programs

*Corresponding author, Associate Professor, E-mail: dqli@dlut.edu.cn

^a Professor, E-mail: [hikli@dlut.edu.cn](mailto:hkli@dlut.edu.cn)

^b Associate Professor, E-mail: renliang@dlut.edu.cn

^c Professor, E-mail: yth@dlut.edu.cn

^d Ph.D., Candidate, E-mail: jjaziguang@foxmail.com

^e MSc. student, E-mail: 930049729@qq.com

to effective and automated monitoring systems.

Traditional manual inspection is labor intensive and could not reveal hidden damages, which are two primary motivations for recent rapid deployments of SHM systems (Pandey *et al.* 1991). Especially in the civil engineering context, many portions of infrastructure built after World War II are approaching or exceeding their design life. Moreover, there are currently no quantifiable methods to determine whether post-earthquake buildings are still safe for reoccupation and whether these structures can continue to serve their purposes need extensive evaluation. The emergence of SHM meets such urgent needs of estate owners and government agencies, and opens a new horizon for civil engineering structures (Farrar and Worden 2013).

However, one cannot be very optimistic for the SHM systems to discover all potential structural damages and to provide instant damage alerts in the short term, not alone to say further maintenance and rehabilitation advices, which are long term perspectives of SHM (Worden *et al.* 2007). In the current stage, damage detection and locating can be realized at a structural component level. Damage quantification is still not fully reliable by the vibration based damage identification methods although they are successful in simulations, laboratory studies and well-controlled experiments (Maeck *et al.* 2001, Roeck *et al.* 2003). During the last two decades, extensive research has been conducted in the vibration-based damage identification, and significant progress has been achieved. Doebling *et al.* (1996) presented an extensive review on the vibration-based damage detection methods up to 1996. Sohn *et al.* (2004) subsequently updated this review on the literature up to 2001. In both the articles, the features for the damage identification were considered to classify various methods. Following closely this classification, Fan and Qiao (2011) presented a literature survey with a particular emphasis on the papers and articles published from 1996 to 2011.

The SHM has undergone great developments in the last decade and attracted many researchers to investigate related issues, including novel sensors (optical fiber sensors (Li *et al.* 2006), PZT sensors, GPS (Li *et al.* 2007) etc.), wireless transmission (Lynch 2007) and energy harvesting (Erturk and Inman 2011), database management and feature extraction (Alvandia and Cremona 2006, Messina *et al.* 1998), damage identification (Peeters *et al.* 2001) and environmental influences, etc.(Ou and Li 2010, Vanlanduit *et al.* 2005). With the development of SHM related technologies and urgent needs of civil infrastructures, many researchers have put the new SHM techniques into engineering practices, including the large-span gymnasium in Dalian carried out by the author's group. This survey tries to give a complete overview of those infrastructures installed with the SHM systems in mainland China. Although many references have been consulted, this review is not meant to be exhaustive and the omission of relevant investigations is unavoidable. However, efforts have been made to ensure this summary review comprehensive and representative of current engineering practice.

This review is organized as follows: Section 2 presents lists of structures installed with the SHM in mainland China, namely high-rise buildings and towers, bridges, large scale sport avenues, offshore platforms, tunnels and dams respectively. Moreover, two typical SHM cases for almost each type of structures are introduced in details as a sample. Section 3 provides a discussion on current challenging issues and potential future trends.

2. Statistics and examples of SHM applications in mainland China

The SHM exercises for high-rise buildings, bridges, large scale sport avenues, offshore

platforms, tunnels and dams are reviewed in this part. Almost all these structures currently installed with the SHM system in China are surveyed. The location, date, features of each project, types of sensors installed and their amounts, and monitoring results or experience gathered from the SHM practices are presented.

In cases, publicized literature doesn't agree with each other on amount of sensors and types for a certain project, which may be due to progressive installation and various upgrade stages. It occurs, of course, that some sensors may turn invalid or fault and cannot function, especially optical fiber sensors are prone to breakage as well known. Therefore, sensors and their amounts are based on papers which are consulted and could not be guaranteed with the current exact ones. Moreover, the SHM is a continuous process and the SHM experience is just a small portion of each project since huge data is going to be further analyzed and more fruitful results will be obtained.

2.1 Large-scale sports venues

A great number of large-scale sports venues have recently been built to accommodate large sports activities, such as the 2008 Olympic Games in Beijing, the 2010 Asian Games in Guanzhou, the 2011 International Swimming Federation World Championships in Shanghai and others.

Table 1 List of large-scale sports venues installed with SHM in mainland China

No.	Project Name	Location / Date	Sensors (Amount)	Monitoring Results	SHM Experience
1	National Aquatics Center('The Water Cube')	Beijing 2003-2008	AnemS (1); PT(26); DispS; FBGT(20); FBGS(230); Acc(26)	Strain ranges within 400µε at upper chords and 300µε at lower chords; Displacement of ETFE cushion ranges within 2mm; Turbulence integral scale is 74.12% along down wind, and 60.11% across wind.	Mode transition and coupling need consideration; Local strains are sensitive to ambient influence.
2	UK Pavilion at the 2010 Shanghai Expo	Shanghai 2010	TS (1);StrainS(20); TAcc(13)	Only slight displacement with 1mm in the vertical direction; Stress with expected range (within 70MPa); Maximum acceleration is within 0.67m/s ² horizontally and 0.33m/s ² vertically.	Accuracy needs improvement due to ambient influences;
3	Dalian Stadium	Dalian 2009	TAcc(24); FBGT and FBGS(200)	Stress varies 12.83MPa at one support while disassembling temporary roof support	Absolute member stress are hard to obtain
4	Dalian Gymnasium	Dalian 2009	TAcc(30); FBGT and FBGS (96); TiltM(24); CFS(48)	A Cable force reaches only 1150kN and compensated later; Inclination angle of the support less than 1.2°	Temperature has to be compensated for accurate force monitoring;
5	Shenzhen Citizen Center	Shenzhen 1998-003	AnemS(2); PT (40); FBGS(12); StrainS(56)	Stress at critical support column are measured; First 4 modes are identified	Limited sensors and absence of effective damage feature
6	Jinan Olympic Center	Jinan 2007-2009	FBGS(150);CFS(48)	Critical member stress and cable force monitored during construction	Wireless sensors are more adaptive
7	Xining Stadium	Xining 2009	AnemS(3); TS(1); StrainS; FBGT(12); FBGS;Acc(26)	Stress and displacement vary not much while disassembling temporary roof support	Stress and displacement shall be monitored simultaneously

Note: abbreviations are listed underneath Table 2

Novel elegant and aesthetic large-space structures are constructed with the development of special structure technique and new material, for instance, the National Aquatic Center (so called as 'The Water Cube') is the largest building in the world built upon "the soap bubble" theory with 3,065 bubble-like pneumatic cushions, and sports a polyhedral steel-framed structure with the ETFE (the ethylene-tetrafluoroethylene copolymer) membrane. In order to assess the new design theory and ensure the safety of large-scale structure construction, a SHM system was installed. On the other hand, similar large-space structures are prone to huge casualties and financial loss if the structure becomes invalid or even collapses under extreme working conditions like storm or earthquake (Li *et al.* 2004). It is therefore urgent to conduct a real-time monitoring system and damage diagnosis on these kinds of long-span special structures. Table 1 is a list of large-scale sports venues installed with the SHM in mainland China, among them Dalian Gymnasium (bold faced) and National Aquatics Center will be presented in more details.

2.1.1 Dalian Gymnasium

Sports center of Dalian in China, which covers an area of 820 thousands square meters and composes of ten venues as shown in Fig. 1, is a comprehensive center of facilities of fitness and recreation for the Dalian citizens and has the capability of hosting major sporting events. The major buildings including the gymnasium, stadium, natatorium and media center, which are typical long-span special structures, were equipped with the real-time SHM system to survey the variation of key physical parameters of structures and provide the real-time alert of structural safety (Li *et al.* 2014).

The overall floorage of Dalian gymnasium is about 81000m², which allows for 18000 spectator capacity with total height of 41 m. The roof structure of which the maximum span is 145.4 m is suspendome structure and shaped like a spheroid. These rings are designed for the prestressed cable system which is consisted of ring cable, radial cable and strut, while the strut made of circular steel tubes adopts the hinged joint and cast steel joint is applied between the cable system and strut. The location of maximum stress was found out based on the FE model results from the ANSYS software as it is shown in Fig. 2(a). More than 200 FBG sensors were installed on the cable anchor, the truss and the strut to monitor the cable force, the stress and the compression stress respectively. The 24 inclinometers were mounted on the base of cable anchor to monitor the angular variation (Jia *et al.* 2011). The 30 accelerometers with three dimensions were fixed on the surface of truss joints to survey the dynamic characteristics of the roof structure. Fig. 2(b) shows the pictures of sensors installed on the roof structure of gymnasium.

(1) Monitoring results of cable system in the prestressing construction

Proper prestress on the radial cable can enlarge the stiffness of the cable system such that the structure would have the ability to undertake external load. Radial cable was tensioned during the construction of the prestressed cable. The whole process was divided into 4 stages: 10%, 50%, 70% and 105% of designed value respectively. In consideration of the quantity of equipment, each stage was carried out group by group to ensure the uniformity of tension. The tension construction lasted for 9 days in the process of which the above system was used to monitor the structure. Parts of monitoring results are listed as followings.

(a) Monitoring results of ring cable

The time-history of C10 cable tension during stretching process is shown in Fig. 3(a). During the first stretching process, the tension of C10 increased from 80 kN to 359 kN. There was a mutation in the process which was caused by the temperature change of sensor as a result of which the temperature compensation was necessary for the sensors.



Fig. 1 Dalian Sports Center

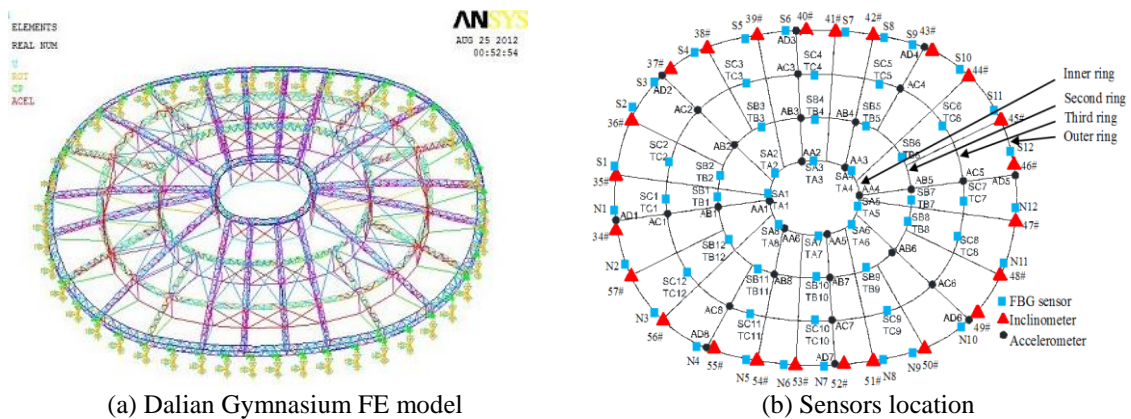


Fig. 2 FE model and sensors location

(b) Monitoring results of strut

The stress time-history of Z1-2 strut in second stage of cable tensioning is given out in Fig. 3(b). In the process of the first stretching stage, the strut pressure stress has increased by 12MPa and 5Mpa during the second stage, because the first stage prestress was directly applied to the radial cable connected with the strut Z1-2 and the second stage prestress was applied to the adjacent radial cable. As a result, the effect of interaction between contiguous cables on strut was significant.

(c) Monitoring results of inclination

The inclination of 34# support increased from -0.888° to -0.851° , which was within the limit $\pm 1.5^\circ$, indicating that the structure was under safe condition, as is shown in Fig. 3(c).

(2) Long-term monitoring results

The monitoring system was switched on from the beginning of prestress construction. Part of the long-term monitoring results acquired by analysis of the monitoring data are as follows.

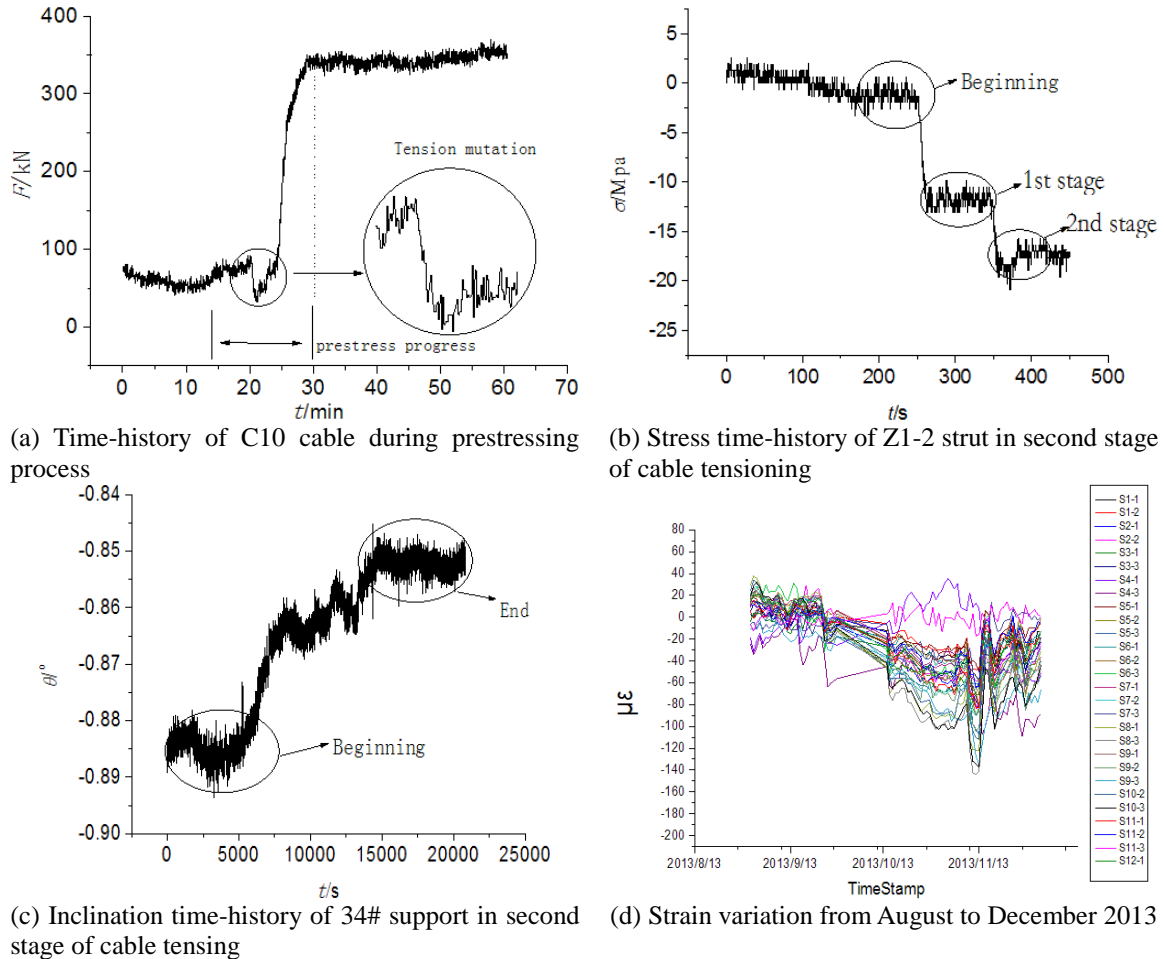


Fig. 3 Monitoring results of cable system in the prestressing construction

(a) Long-term monitoring results

The FBG sensors were installed on the key chord members as shown in Fig. 2(b). Fig. 3(d) shows the strain variation of parts of chord members from late August to early December in 2013. There was nearly no strain variation from August to October. When it came to November and December, the strain was enlarged due to the weight of equipment installed for the concerts and drastically falls in temperature which caused the structural shrinkage inducing the change of strain.

(b) Monitoring results of load tests on roof structure

On October 26th, 28th and 29th in 2013, there were load tests carried out on the roof structure divided into three stages. 20t, 35t and 60t were applied separately, Fig. 4(a). Using the 3D model displaying method, the distribution of strain on the whole roof structure is shown in Fig. 4(b), which indicates that the load application only affected local structure while the entire roof was still under safe condition.

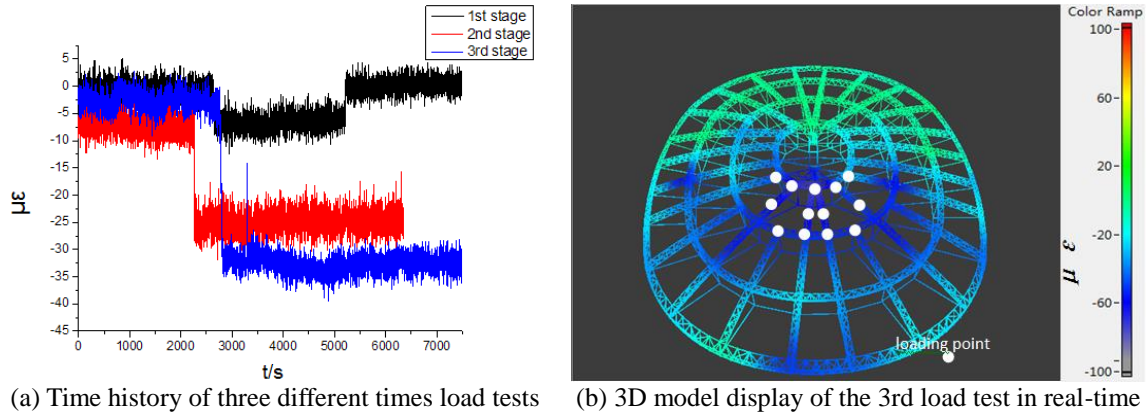


Fig. 4 Monitoring results of load tests

2.1.2 National Aquatic Center for Olympic Games

A SHM system was designed by Ou *et al.* for the Chinese National Aquatic Center, a steel structure covered by the ETFE polymer membrane (shown in Fig. 5). The SHM system is mainly composed by one anemoscope, 26 wind pressure sensors, one laser displacement sensor, 20 FBG temperature sensors, 230 FBG stress sensors, and 26 accelerometers to monitor wind load (wind speed, direction, angle and surface pressure), ambient temperature load (temperature field), strain of critical structural members (upper chords, web member, lower chord and wall member) and vibration of roof lower chords and ETFE cushions (Ou *et al.* 2003).

The SHM system was continuously being operated for the entire duration of the Beijing Olympic Games in 2008. According to the monitoring data, it was discovered that the temperature ranged within 40°C at upper chords and 35°C at lower chords in a day, and that strain ranged within 400 $\mu\epsilon$ at upper chords and 300 $\mu\epsilon$ at lower chords. The displacement of ETFE cushion ranged within 2 mm. The wind turbulence integral scale was 74.12% along down wind, and 60.11% across wind. The wind pressure correlation beyond 20 meters fell almost to zero (Lu 2010). Moreover, ambient vibration techniques (ERA+NExT method) were used to determine dynamic properties (first 4 modes) and global characterization of building as well as the vibration of building under earthquake and wind.

Fig. 5 Structure of the National Aquatic Center for Olympic Games (Ou *et al.*2003)

The authors further discussed the significant change induced by the variation of temperature in intrinsic forces. From the monitored temperature variation in the winter of 2006 and the summer of 2007, it was found that the strain increased with decreasing temperature and vice versa. The maximum variation in strain reached to about 400 MPa when considering the temperature influences. The measured data during construction was suggested to be served as a baseline for evaluating future changes in the condition.

2.2 Bridges

SHM system is most widely applied for bridge monitoring in China. It overshadows the SHM applications in other structures to the degree that the SHM means in a default bridge SHM when the SHM is mentioned and no structure is specified (Aktan 2009, Salawu *et al.* 1995, Sohn *et al.* 1999).

82 bridges currently installed with the SHM system in mainland China were surveyed as shown in Table 2. Abbreviations are used to shorten the table and listed underneath. In fact, many SHM systems can only obtain single measurements, such as the maximum strain at the top or bottom deck, maximum deflection at the mid-span, certain cable forces, extreme stresses, maximum settlement. Many of these partial measurements are all called the SHM system as a fashion. How to combine those single measurements to get a whole picture of the bridge health is still an important issue.

Table 2 List of bridges installed with SHM in mainland China

No	Project Name	Location / Date	Type	Span(m)	Sensors (Amount)	SHM Experience
1	Baling River Bridge	Guangzhou 2009	Susp	1088 (1584)	UW(4);HT(1);FBGT(30);TAcc(2); WIN(2); CFS(64); FBGS(44); TiltM(8); GPS(9); Acc(9);DispS(20);DVC(7)	Member temperature and expansion joint displacement varies with sun angle;
2	Binzhou Yellow River Bridge	Shangdong 2001- 2003	CableS	300 (1698)	GPS(3);AnemS (2); Acc(39);FBGS and FBGT (96).	Wind speed and angle at tower and bridge deck differs not much, Cable forces identified
3	Caiyuanba Yangtze River Bridge	Chongqing 2003- 2007	Tied-arch	420 (800)	StrainS(112); DispS(46); Acc(40); TempS(64); CFS(68)	Tie bar cable force does not exceed the limit.
4	Chongqing Yuao Light Rail Bridge	Chongqing 1999- 2001	RF	160 (352)	Acc(12); TempS (44);StrainS (52);DeflM(11)	Sampling only at certain extreme states to avoid huge data
5	Dongfeng Street Overpass	Jilin 2008	BG	29 (408)	StrainS(48);TempS (14); Thermometer(1);Hygrometer(1);	About 60% of total strain is caused by concrete creep and shrinkage
6	Dafosi Yangtze Bridge	Chongqing 1997- 2002	CableS	450 (1168)	StrainS(40);DT(14);DeflM (42); DispS (4); Acc(20);CFS(97)	Deflection shows cyclical fluctuations similar to the temperature change.
7	Donghai Bridge	Shanghai 2002- 2005	CableS	420 (32.4km)	GPS(3);ExtM(4);CFS(8);StrainS(48); FatM(24);TempS(46);AnemS (3); WaterPG(76);Acc(29);COR(36)	Four layer evaluation system to reduce redundant data
8	Dalian North Bridge	Liaoning 1984- 1986	Susp	132 (230)	GPS(6);Acc	Frequency measured by GPS agrees with Accelerometers
9	Erqi Yangtze Bridge	Hubei 2008- 2011	CableS	616 (1732)	AnemS(5);HT(2);TAcc (3);ASM(8); DT(84); StrainS(173); DeflM(24);	Six evaluation sub-system was designed for different purposes

					TiltM(6); GPS(6);DispS(6);Acc (23);CFS(32); DVC (24)		
10	Wujiang Second Bridge	Chongqing 2004- 2009	CableS	100+340+150 (590)	Acc(5);DeflM(10);FBGS(52);FBGT(28); TiltM(2);CFS(8);Crack meter(4)	Sensors positions at Maximum modal displacement needs consideration	
11	Dongbao River Bridge	Guangzhou 2009- 2012	CableS	120+216+120 (456)	Acc; HT; AnemS;DeflM; PLevel	-	
12	Guantouba Bridge	Gansu 1984- 1988	Susp	180 (213)	AnemS(1); TempS (8); DispS(10); StrainS(56);Acc(14)	Deflection tends to be stable after many years usage.	
13	Huai'an Bridge	Jiangsu 2003- 2005	CableS	152+368+152 (674)	FBGS(32);TotalS(1);Acc(25);DispS(2); StrainS(238)	-	
14	Songhua River Bridge	Heilongjiang 2001- 2004	CableS	336 (1268)	AnemS(1); FBGT;FBGS;Acc(9)	Performance of FBG sensors is stable after two winters and summers	
15	Hongfeng Lake Bridge	Guizhou 2002-2004	CableS	30+102+185 (317)	TiltM(1); Acc(8);FBGT(10);FBG S(13);TotalS(1)	Cable force are identified with measured acceleration	
16	Haierwa Bridge	Hebei 2007	Arch	138 (178)	ASM(2);TempS(2);PLevel(10); DeflM; Acc(18);StrainS(60);AnemS(1)	-	
17	Hulan River Bridge	Heilongjiang 2001	BG	(42) 420	StrainS;FBGS(15);FBGT	Box girder's tension is well monitored by FBG sensors while strain gauge drift	
18	Humen Bridge	Guangdong 1997	Susp	888 (4606)	StrainS(24); GPS(7)	Displacement ranges within 3cm horizontally and 6cm vertically	
19	Hemaxi Bridge	Guangdong 2006	CableS	125+230+125 (1895)	TotalS(1); StrainS(51);Acc (8);CFS (1); TempS(62); HT(4)	-	
20	Huangpu Bridge	Guangdong 2004- 2008	Mixed	1108 (7016)	TempS(3);AnemS(3);WIM(1);GPS(13); StrainS(133);Acc(28);CFS(16);DeflM(2 0)	Cohesion of monitoring system and traffic engineering comprehensive monitoring system is very important.	
21	Hangzhou Bay Bridge	Zhejiang 2003- 2008	CableS	908 (35km)	GPS(8);DeflM(41);Acc(57);StrainS(100);CFS (29);TempS(2);TiltM(7)	The horizontal displacement of GPS is more precise.	
22	Hangzhou Zhijiang Bridge	Zhejiang 2008- 2013	CableS	116+246+116 (1724)	TiltM(20);Acc(48);StrainS(176);TempS (60);PT(16);GPS(4);AnemS(2);WS(1); HT(10)	System is complete and in operation	
23	Hongcaofang Overpass	Chongqing 2000	RF	30 (210)	StrainS(8);DeflM(4);Acc(4)	Deflection cycles in 24 hours	
24	Jiujiang Bridge	Guangdong 1985- 1988	CableS	320 (1675)	CFS(36);StrainS(30);HT(2)	Cable forces and deck strain varies with temperature.	
25	Jinan Yellow River Bridge	Shandong 1978- 1982	CableS	40+94+220+94+ 40 (2023)	GPS;Acc;FBGS;DT	Long distance cabling increase noise level and asynchronous sampling worsens modes	
26	Jiangyin Bridge	Jiangsu 2004	Susp	1385 (3071)	Acc(72); CFS(14); TotalS(1); FBGS;DispS; GPS;HT;AnemS ; Baroceptor	Upgrade old SHM system	
27	Jingyue Bridge	Hubei 2006- 2010	CableS	100+298+816+8 0+75+75 (4302)	DeflM(38);FBGS(824);FBGT(530); Acc(90);CFS(56);MagA(14);GPS(5);Til tM(4);TAcc(4);WS(1)	Maximum stress at top steel deck is -100Mpa, and -8.0Mpa for concrete section	

28	Liaohe Bridge	Liaoning 2001	BoxG	436 (3326)	FBGT(16);FBGS(20);TempS(2);StrainS(20)	Max strain at bottom deck is 28 $\mu\epsilon$ and -11 $\mu\epsilon$ at top, agrees with design values
29	Luohe Bridge	Shanxi 2002- 2006	RigidF	3 x 160 (1056)	PLLevel;DeflM;StrainS;Digital crack monitor	Max settlement is 0.41mm and crack less than 0.33mm
30	Liugang Bridge	Guangdong 2010	BoxG	160	StrainS;TempS	Strains separated by wavelet can reflect various trends
31	Lupu Bridge	Shanghai 2000	Arch	550 (3900)	DT;DeflM;FBGS;Acc	Using optical fiber to transmit data for 5km
32	Maocaojie Bridge	Hunan 2002	Susp	368 (7580)	WIM(2);AnemS(1);TempS(14);FBGS(40);FatM(40);Acc(64)	Optimal sensor placement can reduce SHM cost.
33	Mingzhou Bridge	Zhejiang 2008	Arch	450 (1250)	CFS(22);Acc(15);TempS(40);UW(1);ASM(1);HT(1);DispS(4);DVC(2);GPS(3);StrainS(47);TAcc(2)	Signal types by various sensors are not compatible
34	Nancang Bianzuzhan Bridge	Tianjin 2005	CableS	150+150 (1060)	CFS;Acc;GPS;AnemS;ASM;HT;FBGT	-
35	Nanjing Yangtze Bridge	Jiangsu 1960	Rigid F	1576 (6772)	DispS(20);StrainS(50);Acc(56);TempS(20);AnemS(1);WIM(2);Seismograph(1);TotalS(1)	FEM model updated with identified modes and fatigue damage is accumulating
36	Third Nanjing Yangtze Bridge	Jiangsu 2005	CableS	648 (4744)	AnemS(2);UW(3);HT(3);PT(84);DispS(12);TiltM(48);FBGT(336);FBGS(790);TAcc(4);Acc(21)	Axial force is -90.0MN.
37	Dashengguan Yangzi Bridge	Jiangsu 2006-2009	Susp	336+336 (14789)	AnemS(8);TiltM(16);TempS(10);HT(1);UW(8);PLLevel(8);TAcc(36);StrainS(36);Acc(38);DeflM(8);DispS(16)	Deflection and sediment should be major SHM concerns.
38	Poyanghu Bridge	Jiangxi 1997	CableS	318 (3799)	FBGT;FBGS;GPS;AnemS;CFS;DispS;HT	Cable force identification influenced by other devices
39	Qingcaobei Bridge	Chongqing 2010	Susp	788 (1719)	FBGT(118);HT(1);AnemS(1);FBGS(118);DispS(19);CFS(12);Acc(16)	Sensor positions should be based on bridge response
40	Qingdao Bay Bridge	Shandong 2006-2010	Susp	1300 (28040)	UW(2);GPS(3); TiltM(4);FBG(16);FBGS(22); TempS(2);CFS(22);DispS(4); Acc(28); StrainS(38)	Noise contaminates data precision.
41	Fourth Qianjiang Bridge	Zhejiang 2002- 2004	Tied-arch	190 (1376)	Acc(8);StrainS(50); AnemS(1);TempS(32);TS(1);Magnetic bomb instrument ME(35)	Long cabling increase noise level and causes signal loss.
42	Qinglinwan Bridge	Zhejiang 2007-2010	CableS	380 (10326)	Acc(25); WIM;Disp(4); HT(1); TempS(30);PT(24);UW(1);DVC(2);StrainS(52);TiltM(8);TAcc(2);ASM(1);GPS(2)	Wireless data transmission system avoids cabling.
43	Qingshuiyu Bridge	Zhejiang 2007-2011	CableS	468 (908)	Acc;StrainS;GPS; TempS; CFS	-
44	RunYang Yangtze Bridge	Jiangsu 2000-2005	Mixed	1490+406 (35660)	Acc(173);StrainS(132);TempS(64);GPS(16);AnemS(2)	Cable force, horizontal and vertical displacement, modes
45	Shibangou Yangtze Bridge	Chongqing 2005- 2009	CableS	450 (975)	TiltM(11);DispS(4);FBGS(17);FBGT(17);Acc(17);DVC(8); Crack monitor(4)	Deflection monitored with measured slope
46	Ebian Dadu	Sichuan	Arch	138	FBGS(30); StrainS; GFRP-FBG smart	Bar strain and stress were

	River Bridge	1995		(206)	bar(16)	measured
47	Dongying Yellow River Bridge	Shandong 1987	BoxG	220 (2743)	Acc(29);FBGT(200);FBGS(185)	First 10 modes identified by SSI. Temperature influence and traffic loads analyzed.
48	Sutong Yangtze Bridge	Jiangsu 2003- 2008	CableS	1088 (8206)	AnemS(4);WIM(2); TempS(137); HT(9); TiltM(6);COR(22); GPS(14); DispS(12); Acc(34); StrainS(331);FOS(12); CFS(12)	Deflection, strains etc monitored. Wavelet packet energy used for damage identification
49	Xiaogou Bridge	Shanxi 2003	RF	5×100 (820)	FBGS(73); DeflM(22); TempS(116); ASM(2); Acc(4)	SHM system functions well
50	Shenzhen Bay Bridge	Guangdong 2003- 2007	CableS	180 (5545)	Acc(30);AnemS(5); DispS(5); CFS(25); WIM(2);HT(1); TAcc(1);TempS(27); GPS(4);StrainS(284);Rain gauge(1)	Deflection, forces, boundaries to update actual cable forces
51	Taian Yangtze river bridge	Sichuan 2003- 2008	CableS	208+270 (1573)	TiltM(18);StrainS(280); TempS(140); DeflM(26)	Load tests show that measured data agree with designed values
52	Haihe River Bridge	Tianjin 2001-2002	CableS	310+190 (2838)	AnemS(2);HT(18);FBGS(91); FBGT(79);Acc(23); GPS(3); CFS(26); DispS(4); TiltM(18); COR(2);DVC(4)	Deflection, cable forces, stress and modes are monitored
53	Yonghe Bridge	Tianjin 1987	CableS	260 (512)	HT(1);AnemS(1);CFS(88);TempS(1);G PS(3);Acc(15);ASM(1)	Wireless accelerometers agree with wired ones
54	Tongshunlu Bridge	Beijing	Arch	131	Acc(33);FBGS(70);FBGT(70);TiltM(5); Cable forces are measured and CFS(8)	modes used to update FEM
55	Taizhou Yangtze Bridge	Jiangsu 2007-2012	Mixed	2×1080 (62km)	TAcc(12); Acc(40); StrainS(168); TempS(38); GPS(10)	Local damage can be monitored by local sensors
56	Wuhu Yangtze Bridge	Anhui 1997-2000	CableS	312 (10521)	TempS(24); StrainS(109); DispS(29); Acc(6);DeflM(6);DispS(29); Speed Meter(68)	Maximum bar stress, deflection are used for SHM alarms
57	Wenhui Bridge	Zhejiang 2000-2002	CableS	240 (446)	DispS(11); TempS(12); StrainS(20); Acc(12); DVC(1)	-
58	Junshan Yangtze Bridge	Hubei 1998-2001	CableS	460 (4881)	GPS(3);TiltM(4);AnemS(1);CFS(38);H T(1);WIM(6);FBGS(126);	Deck&tower deflection, stress and cable forces monitored
59	Wuzhong Yellow River Bridge	Ningxia 2010	RigidF	360 (3098)	StrainS(30);FOS(72)	Optical fiber sensors are accurate than strain gauges
60	Xiabaishi Bridge	Fujian 2001	RigidF	2 x 260 (810)	StrainS(62);TS(2);Acc(31);DspS(22)TempS(16);	Long cabling interruption
61	Xinguang Bridge	Guangdong 2004- 2007	Arch	428 (1082)	StrainS(288);FBGS(20); WS(3); Acc(60);GPS(16) ;DVC(6)	Fatigue impossible due to lack of WIM
62	Guozigou Bridge	Xinjiang 2011	CableS	360 (700)	HT(3);AnemS(2);WIM(1);PT(16); StrainS(132);TempS(70);Acc(30); GPS(6);DispS(4);TiltM(12).	Efficient sensor placement and huge data processing
63	Xintanqijiang bridge	Chongqing 2001	RigidF	75+130+75 (280)	TempS(20);WaterPG(5);StrainS(38);Ma gA(4);PT	-
64	Xupu Bridge	Shanghai	CableS	1074	StrainS(20);WIM(1);TempS(20);DeflM(-	

		1994- 1996		(6017)	15);Acc(20)	
65	Xiangshangang Bridge	Zhejiang 2007- 2010.	CableS	688 (1376)	GPS;AnemS	Deflection monitored while storm and shutdown alerts sent
66	Xushuigou Bridge	Shanxi 2007	Mixed	200 (1069)	StrainS(22);PLevel(5)	-
67	Yichang Yangtze Bridge	Hubei 1998- 2001	Susp	960 (1206)	TempS(80);TotalS(28);Acc;StrainS;DeflM	Dynamic strain, deflection and modes were measured
68	Yangluo Yangtze Bridge	Hubei 2003-2007	Susp	2725 (1280)	FBGS(48);DispS(2);GPS(5); Acc(56);FBGT (96);	-
69	Yeqingdou Bridge	Zhejiang 1993	Arch	228	TempS(6);Acc(17);DispS(3);StrainS(16)	Bar force monitored and used in evaluation
70	Yingzhou Bridge	Henan 2009	Arch	610 (1160)	FBGS; DispS(20); StrainS(79);	The maximum main stress of arch rib is 6.671Mpa, and the minimum is -206.772Mpa.
71	Zhaobaoshan Bridge	Zhejiang 1995- 2001	CableS	258 (2482)	AnemS;TempS;StrainS;	SHM data show that bridge is in good working condition.
72	Zhanjiang Bay Bridge	Guangdong 2003-2006	CableS	840 (3981)	TempS(8) ;CFS(16);StrainS(18);TiltM(1))AnemS(3);GPS(3).	Many hardware and huge data
73	Xijiang Bridge	Guangdong 2003	Box G	144 (1624)	StrainS(120);TempS(30)	Overheavy vehicle monitored
74	2nd Zhongshan Bridge	Guangdong 1995	Arch	125 (617)	StrainS(52);TempS (10);AE sensors(19); CFS(10);Acc(7)	-
75	Zhengzhou Yellow River bridge	Henan 2002- 2004	Arch	800 (9848)	Acc;StrainS;AnemS(6); TempS(4);HT(4).	Long cabling
76	Zhengzhou Road-rail Bridge	Henan 2006-2010	CableS	168 (9177)	AnemS(1);CFS(6);Acc(8);PLevel(7); StrainS(18);TempS(16);ExtM(4); ASM(7);HT(1);WIM(4);Speed meter(3)	-
77	Dongting Lake Bridge	Hunan 1996-2000	CableS	310 (5747)	Acc(16); GPS(5);DispS(22); StrainS(28); CFS(16); TempS(21); Speed meter(2)	--
78	Masangxi Bridge	Chongqing 1998-2001	CableS	360 (1104)	FBGS(44); DT(35); DeflM(22); HT(4);Acc(4)	Frequency of four cables varies between 0.9 Hz to 1.1 Hz.
79	Rainbow Bridge	Hubei 1997-2000	Arch	302.93 (990)	CFS(36);PLevel	Cable forces vary synchronously with temperature
80	Sanmenjiang Bridge	Guangxi 2004-2006	CableS	160 (360)	StrainS;CFS;AnemS;Acc;DisS;TempS	--
81	Bachimen Bridge	Fujian 2003	Mixed	520 (3561)	DispS(17);TempS(16); StrainS(35); Acc(16);	Longitudinal displacement are 6.7mm, 6.54mm, 12mm and 12.1mm.
82	Boguan Bridge	Liaoning 2010	Arch	430 (1113)	FBGS(80);FBGT(40);AnemS(1); Acc(32);GPS(2)	-

Abbreviations: Acc- One-way vibration sensor; AnemS – Anemoscopes; ASM- Axle and speed meter; BoxG – Box Girder Bridge; CableS - Cable stayed bridge; CFS- Cable Force sensor; DeflM - Deflection meters; DispS - Displacement sensor; DT - Digital temperature sensor; DVC- digital video cameras; ExtM – Extensometer; FatM - Fatigue meter;FBGS - FBG strain sensor; FBGT- FBG temperature sensor; HT – Hygrothermograph or Thermometer; LVDT - LVDT sensor; MagA- Magnetostriction apparatus; MW - Mechanical wind speed and direction instrument;

PLevel - Precise level; PT -Pressure transmitter; RigidF – Rigid Frame Bridge; StrainS - Strain sensor; Susp – Suspension Bridge; TAcc - Tri-axle accelerometers; TempS - Temperature sensor; TiltM – Tiltmeter or Inclinator; TotalS - Total Station; UW - Ultrasonic wind speed and direction instrument; WaterPG - water pressure gauge; WaveG – Wave gauge; WIM- Weigh-in-motion system; WS- Weather Station; COR-Corrosion meter; FOS-fiber optic sensor; ALS-Anode ladder system; GPR-Ground Penetrating Radar; SPB-soil pressure box;

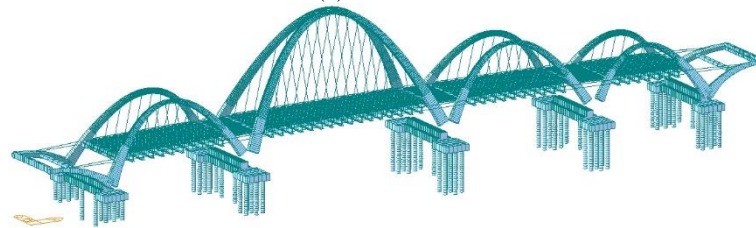
2.2.1 Shenyang Boguan Bridge

The 1113 meters long Shenyang Boguan Bridge crosses the fast flowing Hun River in Shenyang in North Eastern China. The main span of bridge is 430 meters long and 32 meters wide. Shenyang Boguan Bridge is a “ribbon” style bridge with a 67 meters high arch; the parabola shaped structure is the most beautiful bridge to cross the Hun River. Fig. 6(a) shows the overview of the bridge. Shenyang Boguan Bridge is the first half-through 6-span “ribbon” style skew arch bridge in China. To ensure the safety during its construction and service, a complete set of SHM system was designed and installed on it. To perform the dynamic analysis and obtain the vibration characteristics of the bridge, a three dimensional finite element (FE) model was developed using the MIDAS-CIVIL software (MIDAS Information Technology Co., Ltd.), as shown in Fig. 6(b). It contains 6,597 Beam Elements, 174 Truss Elements, 1,518 Plate Element, and 6,365 nodes.

The SHM system architecture of the bridge is configured in four integrating modules comprising the sensor subsystem, data acquisition and transmission subsystem, data management subsystem, and condition assessment subsystem. 1) As shown in Fig. 7, the sensor subsystem comprises five types of sensor: FBG strain sensors, FBG temperature sensors, accelerometers, anemometers, global positioning systems (GPS) receivers. These sensors collect the signals and deliver them to the PC-based data acquisition system through category 5 unshielded twisted-pair cables. 2) The data acquisition and transmission are the PC-based data acquisition units connected by fibre optic network. The data acquisition instruments, the si425 Optical Sensing Interrogator and NI PXI-1044 Chassis, both provide open data acquisition programs based on the LabVIEW platform. But these two data acquisition programs are mutually independent, so the signals of FBG sensors and electrical sensors can't be acquired synchronous. In order to integrate these two data acquisition instruments, the data acquisition programs of NI PXI-1044 were embed into the si425 data acquisition software and developed a synchronous acquisition system for both optical and electrical sensors. By this synchronous acquisition system, the si425 Optical Sensing Interrogator and NI PXI-1044 Chassis could be simultaneously controlled and synchronous data acquisition of optical and electrical sensors is guaranteed. 3) The database manages the construction information, monitoring data and analysis results, which is the core part of SHM system and directly related to the efficiency the whole system. The relational and network database SQL Server 2000 is adopted as the central database of the SHM system. Correspondingly, Database Connectivity Toolkit (DCT), which encapsulates a series of senior function modules, is adopted in this system to access SQL Server 2000. 4) The condition assessment subsystem includes four functions: security warning, model updating, damage identification, and safety assessment. Each subsystem is capable of stand-alone operation under normal and abnormal conditions irrespective of whether they are inter-connected together, i.e., failure of an individual module will have no detrimental effect on the remaining parts of the system.



(a) Overview



(b) Full-scale FE model

Fig. 6 Shenyang Boguan Bridge and its FE model

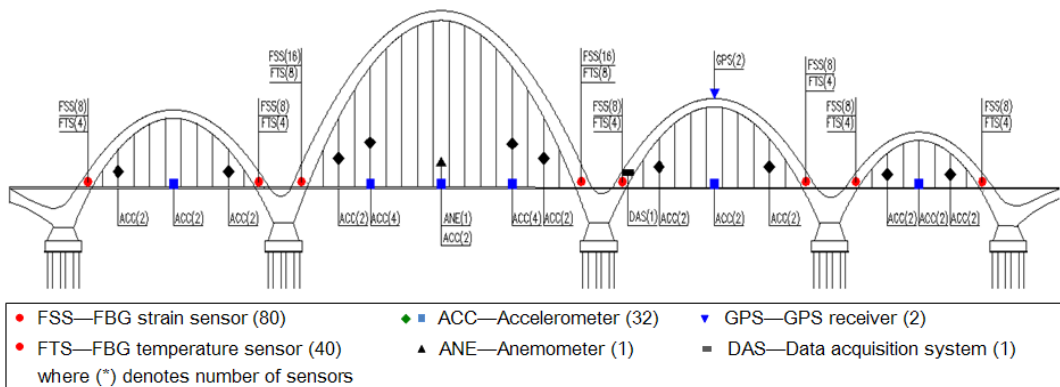


Fig. 7 Distribution of sensors in Shenyang Boguan Bridge

2.2.2 Sutong Yangtze River Bridge

The Sutong Yangtze River Bridge is a cable-stayed bridge that spans the Yangtze River in Jiangsu province (Li *et al.* 2010). It was the cable-stayed bridge with the longest main span in the world in 2008-2012 with a main span of 1,088 meters and two side spans of 300 meters as shown in Fig. 8.

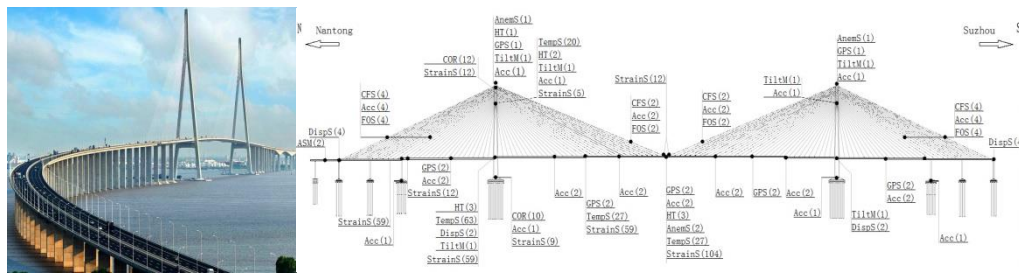


Fig. 8 Sutong Yangtze River Bridge (Li *et al.* 2010)

The bridge received the 2010 Outstanding Civil Engineering Achievement award from the American Society of Civil Engineers. Two towers of the bridge are 306 meters high, and thus it is the second tallest in the world. The tower is an inverted Y-shaped reinforced concrete structure with one connecting girder between tower legs. The bridge deck is a steel box girder with internal transverse and longitudinal diaphragms and fairing noses at both sides of the bridge deck. The total width of the bridge deck is 41 meters including the fairing noses. For such a large bridge, a SHM was installed to continuously monitor its behavior. There are in total 12 displacement sensors, 329 strain sensors, 137 temperature sensors, 32 accelerometers, 8 anemoscopes, 12 cable force sensors, 9 GPS stations, 22 corrosion bars, 6 inclinometers and 2 axle and speed meters installed. Based on the 240-day health monitoring data, it reveals that the seasonal change of environmental temperature accounts for the variation of a damage alarming parameter with an averaged variance of 200%. A 6th-order polynomial is adopted to formulate the correlation between the damage alarming parameter and temperature and abnormal changes of measured damage alarming parameter are detected using the mean value control chart (Li *et al.* 2010). In this way, an environmental-condition-normalized damage alarming method is proved to be suitable for the on line and real-time condition monitoring for the main girder of the Sutong Bridge.

2.3 High-rise buildings and towers

For high-rise buildings and towers, two major concerns are wind loads and earthquake excitations. The aim of SHM for these structures is to provide the information on ground motions and wind pressure loads to assess story-drifts and maximum accelerations at the top floors for the safety of the building and improvement of occupancy comfortability. Table 3 shows a list of high-rise buildings installed with SHM in mainland China, among them Guangzhou New TV Tower and Shanghai Tower (bold faced in Table 3) will be presented in details.

2.3.1 Guangzhou New TV Tower

The Guangzhou New TV Tower (GNTVT), as shown in Fig. 9, is a supertall tube-in-tube structure with a height of 610m (Ni *et al.* 2005). The GNTVT consists of a reinforced concrete inner tube and a steel outer tube with the concrete-filled tube (CFT) columns with 37 floors connecting them. 37 floors serve for offices, entertainment, catering, tour, and mainly emission of television signal. The outer tube comprises 24 CFT columns which are uniformly spaced in an oval while inclined in the vertical direction. The oval decreases from 50 m x 80 m at the ground to the minimum of 20.65 m x 27.5 m at the height of 280 m, and then increases to 41 m x 55 m at the top of the tube (454 m). The columns are interconnected transversely by steel ring beams and bracings.

The inner tube is in oval shape as well with a dimension of 14 m x 17 m in plan, but its centroid differs from the centroid of the outer tube. This hyperbolic shape makes the structure attractive in aesthetics while complex in mechanics.

A sophisticated SHM system consisting of over 600 sensors has been designed and is being implemented for both in-construction and in-service real-time monitoring. There are 16 types of sensors as listed in Table 1 deployed for monitoring of three categories of parameters: (i) loading sources (wind, seismic, and thermal loading), (ii) structural responses (strain, displacement, inclination, acceleration, and geometric configuration), and (iii) environmental effects (temperature, humidity, rain, air pressure, and corrosion).

It is worth mentioning that the monitoring system has recorded the structural responses of the GNTVT caused by several extreme events such as the Wenchuan earthquake, Neoguri typhoon, Kammuri typhoon, and Nuri typhoon during the construction period. The devastating M8.0 Wenchuan earthquake occurred at 14:28 on May 12, 2008 in Sichuan Province of southwest China. All the embedded strain gauges signaled large strain variations lasting for 1–2 min on that day and the maximum stress variation in the cross-sections was 3.6MPa. The measured maximum 3-s gust wind speed at the tower top was 28.1 m/s during the Neoguri typhoon, 32.3 m/s during the Kammuri typhoon, and 25.5 m/s during the Nuri typhoon, respectively. During the three typhoons, the measured maximum acceleration and displacement were close to 0.05 m/s^2 and 15 cm, respectively.

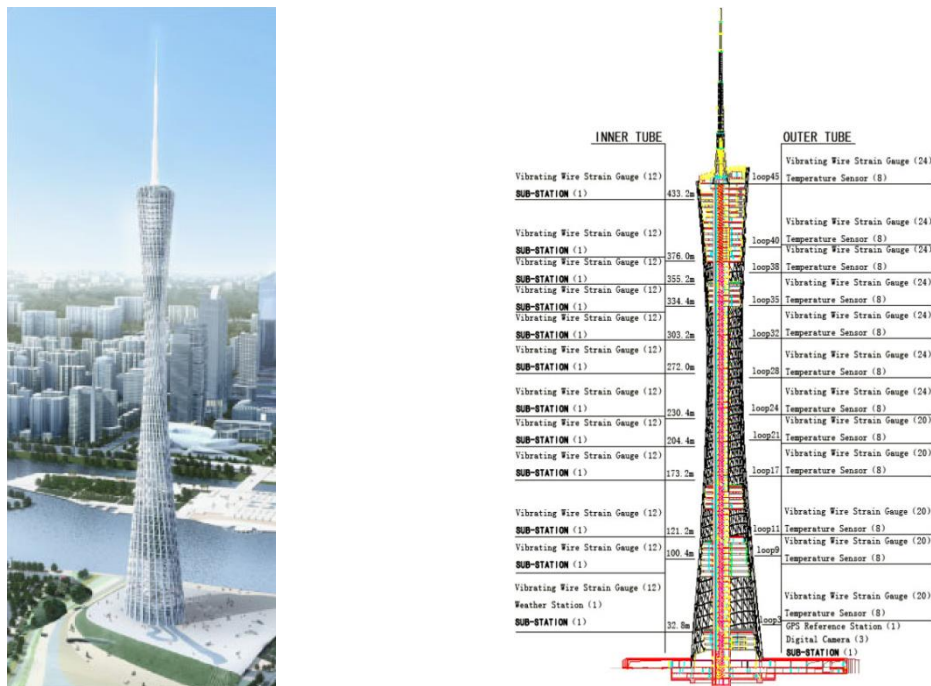


Fig. 9 Deployment of sensors for in-construction monitoring of Guangzhou New TV Tower (Ni *et al.* 2005)

Table 3 List of buildings installed with SHM in mainland China

No.	Project Name	Location / Date	Height	Sensors (Amount)	SHM Experience
1	Shenzhen Vanke Center	Shenzhen 2006-2009	- ²	FBGS(70); FBGT(35); StrainS(154); Intelligent bars(16) ; Acc(14); TS(102)	Obtain the stress distribution of the whole structure based on the limited strain measurements
2	Guangzhou New TV Tower	Guangzhou 2005-2009	600 m	WS (1); AnemS(2); PT(4); TotalS(1); Zenithal telescope(2); TiltM(2); GPS(2); StrainS(416); PLevel(2); Theodolite(2); TH(96); DVC(3); Seismograph(1); COR(3); Acc(22); FOS(120);	Measured strain changes from $-188\mu\epsilon$ to $-184\mu\epsilon$ during the Wenchun earthquake; Measured acceleration ranges is $0.05/s^2$ and measured displacement 15cm during a typhoon
3	Yangtze crossing Campaign Memorial	Hefei 2008-2012	-	Stress meter(244); StrainS (27); Steel bar gauge(29);	Bar stress of the upper chord and the lower chord changed not much
4	Guangzhou International Finance Center	Guangzhou 2005-2009	432 m	GPS (2); AnemS	Wind speed ranges from 0m/s to 9m/s; Frequency in X and Y direction are 0.1484Hz and 0.1523Hz
5	Leatop Plaza	Guangzhou 2007-2011	303 m	Acc; GPS; AnemS	Wind speed ranges from 5m/s to 20m/s; Acceleration is about $0.01m/s^2$;
6	Shanghai Tower	Shanghai 2008- 2015	632 m	Seismograph(2); AnemS(2); PT(27); Acc(71); TiltM(40); TH(75); StrainS (209); GPS(3); TotalS(2); PLevel(1); DVC(1)	Max horizontal displacement was 13mm eastward and 26.5mm southward
8	Jinmao Tower	Shanghai 1994- 1999	420.5 m	TiltM; Acc; GPS; Seismograph	Identify modes in 3 years;
9	Changde Apartment	Shanghai 1936	8 Fls (Historical Building)	FBGS(7)	Strain trend from 3rd Dec 2004 to 26th July 2005; Crack early-warning curve.
10	Shanghai Great World	Shanghai 1924	9 Fls (Historical Building)	Acc; TempS	First frequency structure is 1.7Hz and is not sensitive to temperature variation.

Note: abbreviations are listed underneath Table 2

2.3.2 Shanghai Tower

The Shanghai Tower is the tallest building in China with a structural height of 580 m and an architectural height of 632 m (Su *et al.* 2013). It adopts a mega-frame-core-wall structural system, which consists of a core wall inner tube, an outer mega-frame, and a total of six levels of outriggers between the tube and the frame (Hu *et al.* 2014). A triangular outer facade encloses the entire building, which gradually shrinks and twists clockwise at approximate 120° along the height.

A sophisticated SHM system was being installed to monitor the strains and stresses at critical components, the deflection and settlement of the entire structure, and the structural performance of the building under extreme loadings during construction and service stages, which are the main concerns of the designer, the contractor, and the client. The SHM system consists of more than 400 sensors with 11 different types as shown in Table 1. These sensors are deployed to monitor three categorical parameters: loadings (wind pressure, structural temperature, and earthquake), structural responses (settlement, inclination, displacement, strain, and acceleration), and environmental effects (ambient temperature and wind). The layout of sensors is illustrated in Fig. 10.

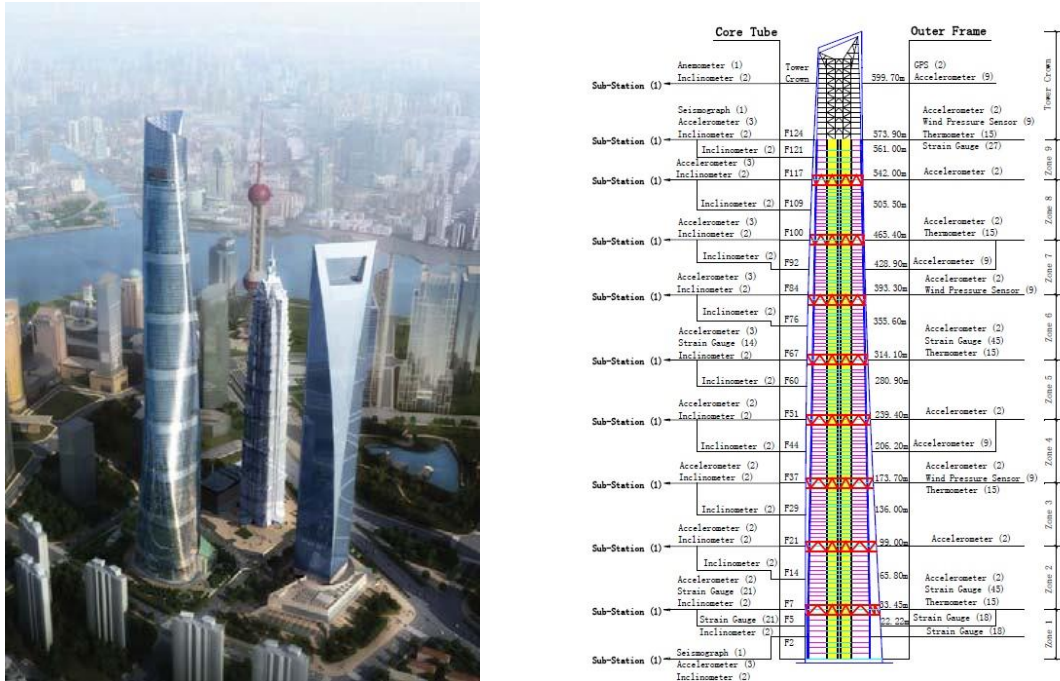


Fig. 10 Sensor layout of the Shanghai Tower (Su *et al.* 2013)

During construction, a total station and a digital level were employed to monitor the settlement of the foundation and the upper floors. The total settlements of the foundation floor at different locations were generally in close agreement with a difference of 8 mm, which indicates that the foundation has no significant non-uniform settlement. The GPS stations and a total station were combined to measure the horizontal displacement at the top of structure. It was observed that the temperature-induced horizontal displacement had a maximum value of approximate 30 mm at a construction height of 180 m. Furthermore, the monitored compressive stresses gradually increased along with construction progress and the stresses at all points were rather small compared with the material strength. Now the SHM system is working in the service stage and more meaningful result will appear.

2.4 Offshore platforms

Seven offshore platforms were installed with the SHM system as shown in Table 4 and Fig. 8. They are the Challenger Deep Sea Floating Platform in the South China Sea and the JZ20-2MUQ Platform in the Bohai Sea. It can be seen that ocean environmental loads, especially ocean wave, current and ice forces, are major concerns for offshore platform structures (Ou *et al.* 2001). Correspondingly, the sensors used in offshore platforms are quite different from those used in buildings and bridges.

Table 4 List of offshore platform installed with SHM in mainland China

No.	Project Name	Location / Date	Sensors (Amount)	SHM Experience
1	The Challenger Deep Sea Floating Platform of South China Sea	South China Sea 1995	AnemS; Radar wave detector; Current meter; Barometer; Tension sensor; Mooring measurement device; PT; StrainS; Acc; GPS; Inertial navigation system; Angle sensor	On-line and acoustic transmission sensors are not applicable under water
2	JZ20-2MUQ Platform of Bohai Sea	Bohai 2010	AnemS; Angola's current meter; Ice pressure box; DVC;	Base transverse force changed little in January 1991 and large in January 2001
3	JZ20-2NW	Bohai 2005	Acc(3+3); DispS(4)	The greater the vibration, the faster structural vibration attenuation.
4	JZ20-2MSW	Bohai 1997	Acc	-
5	JZ9 — 3	Bohai	Acc; Ice pressure box; DVC; StrainS;	-
6	No. CB271	Bohai 2004	FBGS; StrainS;	FBG strain sensors over lived than stain gauges; Ship collision and ocean wave loads are monitored
7	No. NB352	Bohai 2006	FBGS(40); FBGT(6);	Process of lifting tasks and variation of loads of upper structure are monitored

2.4.1 CB271 monopile offshore platform

The FBG sensors were applied to the strain monitoring of oil production offshore platform No.CB271, located in the Bohai Sea of China. At the bottom of central pillar, three bare FBG sensors were placed as a strain rosette on the surface of pillar, and an FBG temperature sensor was placed close to those strain sensors for the temperature compensation. One year later, after this offshore platform had been built in the sea area of oil extraction, the FBG sensors installed in the bottom of central pillar were working well as expected, and did not show any significant reduction of sensing performance. However, the strain gauges placed near the FBG sensors failed to operate due to the detrimental corrosion of seawater (Fig. 11). In this aspect, the FBG sensors demonstrated distinct advantages for the long term health monitoring of ocean structures because of their reliability and durability.

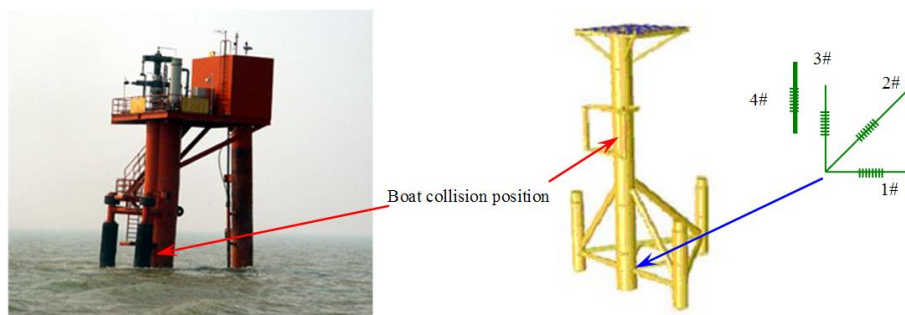


Fig. 11 Platform picture, model and sensors position

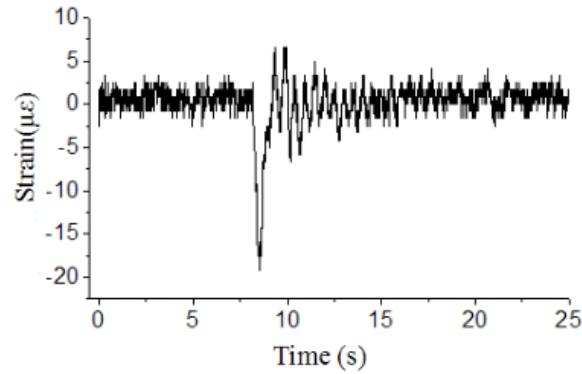


Fig. 12 Strain course induced by ship impact by embedded FBG stain sensors

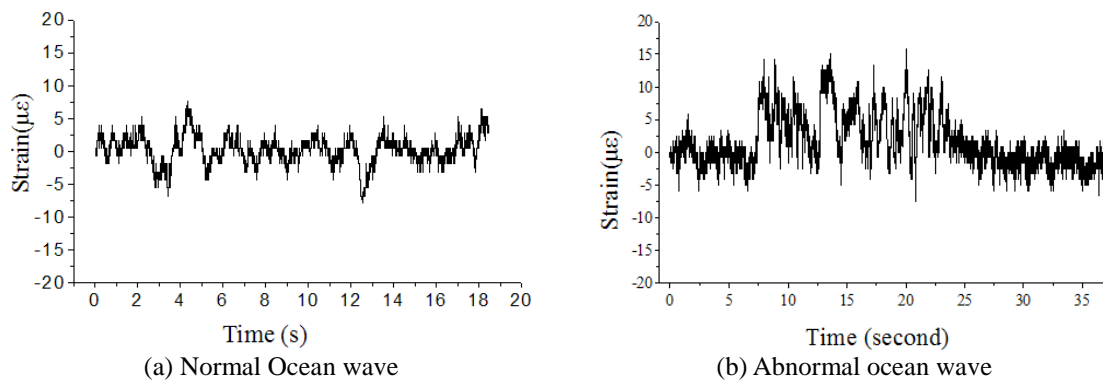


Fig. 13 Strain course induced by ship impact by embedded FBG stain sensors

(a) Ship collision

Supplying boat collision is one of the most critical accidents that can affect the structural safety of offshore platform and the integrity of fixed installation (Visser 2004). It is, therefore, significant to monitor the real-time strain variation of ship collision. In Fig. 12, a strain course induced by an impact of ship with hundreds tons weight was recorded by the FBG sensors in July, 20, 2004. Fig. 11 exhibits a position of ship collision in this offshore platform. Three FBG sensors placed as a strain rosette in three different directions are $\alpha_1=0^\circ$, $\alpha_2=45^\circ$ and $\alpha_3=90^\circ$ respectively. The maximum principal strain is $-27.7 \mu\epsilon$ and its direction is 251.3° . For this strain was in the range of platform linear elasticity, this boat collision did not bring any potential damage to the ocean platform.

(b) Ocean wave loads

Ocean wave is another critical factor that can influence the structural health of an ocean platform. The strain variation of offshore platform in the Bohai Sea induced by normal ocean wave loads was monitored by these FBG strain sensors as shown in Fig. 13(a). In the course of strain measurement, these FBG sensors monitored an abnormal process of ocean current impact, which lasted about 20 seconds as shown in Fig. 13(b). The intensity of this ocean current was

apparently greater than the normal ocean wave presented ahead. Comparing the maximum strain of ship collision with the ocean wave, the intensity of later was not much less than the former. The influence of ocean wave impaction cannot be negligible during the period of oil ocean platform operation.

2.4.2 Offshore jacket platform

An oil production offshore jacket platform in the Bohai Sea of China was instrumented with 40 FBG sensors and monitored for the piles loading under the condition of platform construction and operation as it is shown in Fig. 14. The aim of this study was to provide a realistic assessment of integrity of the foundation piles for future use. The stress loads in the pile heads were transferred from the total weight of the upper structure of platform through the six piles. The weight variation of the upper structure of platform would cause the elastic deformation of six upright piles and be monitored in real-time by the FBG strain sensors installed in the surface of piles. To eliminate the stress bias influenced by the buckling stress and the eccentricity of piles, every 4 FBG strain sensors were mounted on each pile evenly along the pile hoop as it is shown in Fig. 14. In addition, one FBG temperature sensor was installed in each pile to compensate the stress shift of temperature variation.

After the sensors and the demodulation system installation, a calibration test for the system commissioning was carried out to investigate the effectiveness of SHM system. A series of lifting tasks were executed in one and a half hours by the run-operator of platform to convey the equipment of drilling from the transportation ship to the platform. The whole process of lifting tasks was monitored in real-time by the SHM system and the loading result agreed well with the record provided by the crane as it is shown in Fig. 15. It can be seen that there were seven wave crests in the Fig. 16 which happened in the pile B3 and apparently induced by the cargo lifting and discharging process of crane. The Fig. 17 presents the variation of total weight of upper structure of platform in two months monitored by the SHM system. It can be drawn that this offshore platform was under safe condition for that the maximum load of the upper structure platform and the pile heads were separately about 73% and 40% to 70% of the total weight which was much less than the alert load that is 85% of the total weight.

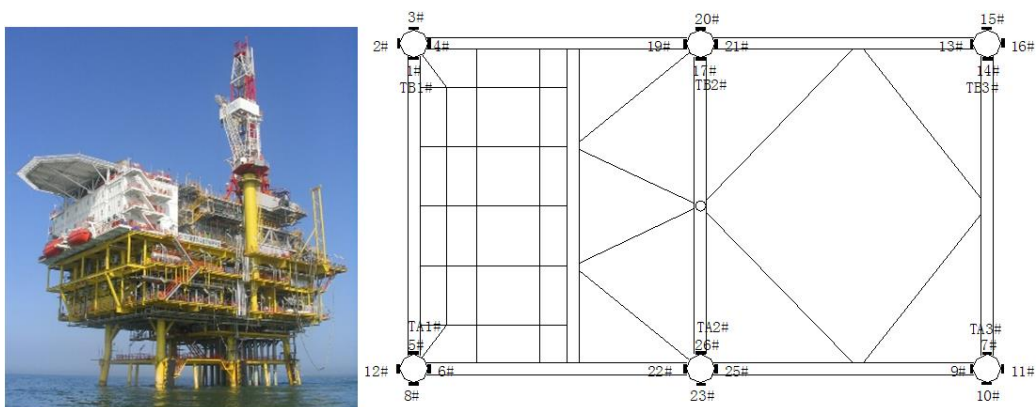


Fig. 14 Offshore platform and position of FBG sensors on piles of platform

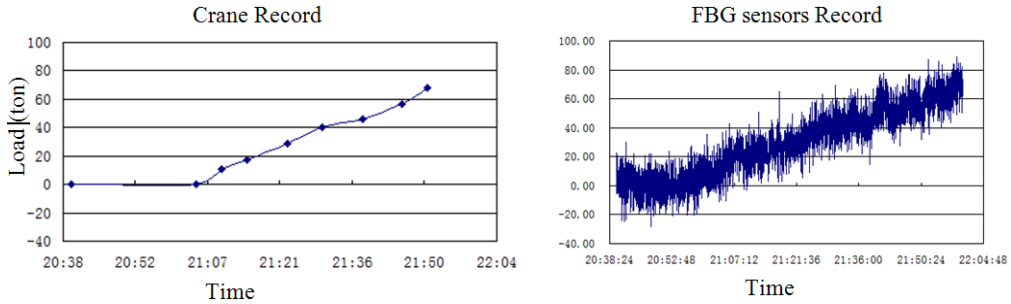


Fig. 15 Process of lifting tasks and variation of loads of upper structure

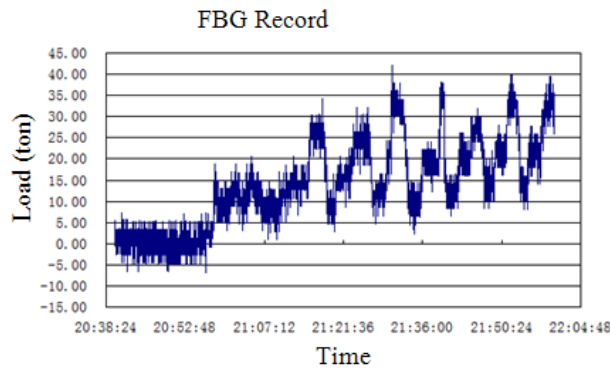


Fig. 16 Variation of loads of pile B3

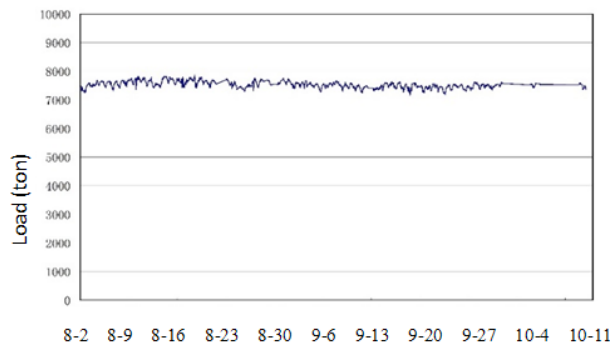


Fig. 17 Variation of total weight of the upper structure

In this project, the SHM system based on the FBG sensors exhibits its unique advantages in the field of offshore engineering ranging from its long-term durability, good reliability, immunity to EMI and well flexibility of installation. Further work should be conducted to overcome the shortcomings of FBG sensors exposed in this project such as the strain bias induced by the effect of temperature variation, anticorrosion measures and optical signal distortion.

2.5 Underground facilities

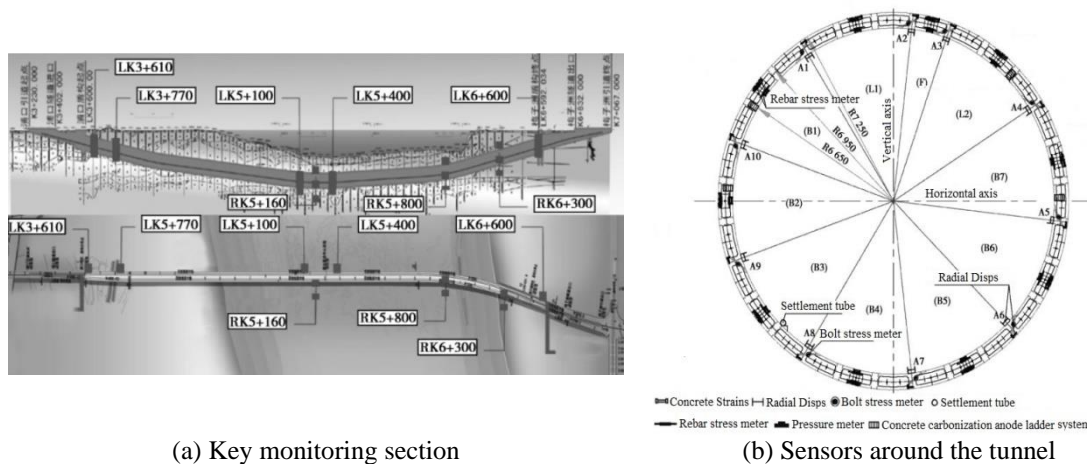
The majority of SHM related researches completed to date have focused exclusively on ground structures. A Singaporean researcher addresses major technological issues and challenges associated with the structural monitoring of underground structures (Bhalla *et al.* 2005). For underground structures, critical regions are usually inaccessible for visual inspections. Additionally compared with the structures on the ground, there are numerous considerations specific to these underground structures such as earth pressures, ground movements and ground water fluctuations and thus brings difficulty to predict accurately at design stage. Table 5 is a list of tunnels installed with the SHM in mainland China, among them the Nanjing Yangtze River Tunnel and Shanghai Expo Power Tunnel (bold faced) will be presented in more details.

2.5.1 Nanjing Yangtze River Tunnel

The Nanjing Yangtze River Tunnel is the first underwater crossing of the Yangtze River in Nanjing, Jiangsu Province (Min *et al.* 2015). The tunnel provides a 6-lane highway crossing as supplement to the existing busy and congested bridge crossings. The overall length of the tunnel is 5859 m, consisting of a 3020 m slurry shield tunnel from the north of the river to Jiangxin Island in the middle of the river, joined by a 2739 m bridge leading to the south main city. The tunnel and the bridge are designed to have bidirectional six lanes. The tunnel is constructed with two slurry shields with the diameter of 14.93 m.

Table 5 List of tunnels installed with SHM in mainland China

No.	Project Name	Location / Date	Length(m)	Sensors (Amount)	SHM Experience
1	Nanjing Yangtze River Tunnel	Jiangsu 2010	6042	DispS; FBGT; SPB; Osmometer; FBGS; PT; WaterG; Multibeam echosounder; PLevel; Laser Profiler; GPR; ALS; StrainS;	Sensors need to have good waterproof, moistureproof, anticorrosive, long-term durability, strong anti-jamming capability
2	Guanggan Highway Tunnel (Dujiaoshan Tunnel)	Sichuan 2012	1833	StrainS(90)	Concrete strain at typical tunnel sections are monitored
3	Xiangan Tunnel	Fujian 2010	4200	Osmometers(24); PT (112); DispS(6); Water Level(1); Seismograph(1); FBGS(369);	Sensor needs seawater and salt fog corrosion prevention measures.
4	Shanghai Dapu Road Cross-River Tunnel	Shanghai 1971	2760	FBGT; FBGS; Crack meter	Circumferential gap were monitored
5	Yongjiang Tunnel	Fujian 1995	1019	PLevel; DispS; Crack meter; StrainS; FBGS; COR	Largest deformation occurs in the roof and bottom of the horizontal section and maximum stress is on the roof (bottom) board or the corner points
6	Beijing Guomao Subway Station	Beijing 1999	-	FBGT (10); PT(10); Osmometer(10); FBGS (39); DispS(15); Laser Profiler; ALS	Train travelling has little influences on the stress of the subway station
7	Nanjing Yangtze River Tunnel	Jiangsu 2009	5853	FBGT; FBGS;	Structural responses were within threshold values and safe.
8	Nanjing Gulou Tunnel	Jiangshu 1994	1150	FBGT; FBGS;	Maximum crack opening of the tunnel in west is 0.142mm
9	Shanghai Expo Power Tunnel	Shanghai 2010	15250	Water Level; Cracks and joints opening meter	Maximum differential settlement is 4.475mm



(a) Key monitoring section

(b) Sensors around the tunnel

Fig. 18 SHM system of the Nanjing Yangtze River Tunnel (Liu *et al.* 2011)

In the project, the most difficult tunnel with a giant size across the Yangtze River, several construction difficulties exist, such as the opening chamber under high pressure and under-passing the section of super shallow cover under the Yangtze River. Therefore, a SHM system was designed to monitor the complex construction and operational safety. The system consists of connecting tube profile monitors, FBG tiny displacement sensors, FBG temperature sensors, FBG soil pressure boxes, FBG Osmometers, FBG bar strain sensor, FBG concrete strain sensors, laser profiler, ground penetration radar and anode ladder system to monitor the structural strains, environmental temperatures and loads including the soil pressure, water pressure and traffic as shown in Fig. 18. All parameters can be viewed in the control room and alerts will be issued once certain values exceed preset thresholds (Liu *et al.* 2011). The SHM system functions well and the Nanjing Yangtze River tunnel was successfully completed through a highly permeable gravel stratum under the water pressure of 0.65 MPa and opened in May of 2010.

2.5.2 Shanghai Expo Power Tunnel

Shanghai Expo Power Tunnel has a length 15.25 km and the maximum tunnel diameter is 6.2 meters. It is a part of planned 200 km power tunnel for continuous development of Shanghai urban construction. Power cables and affiliated facilities are very sensitive to water. Therefore, curvature and height difference have to be controlled to avoid water leakage and structural corrosion for the protection of oil-filled cable. Xie and Feng (2012) developed a real-time health monitoring system for a power tunnel with the key issue of measuring the joint deformation which was an indicator of water leakage when large deformation occurred. As shown in Fig. 19, the SHM system mainly consists of three monitoring items: (i) Differential settlement monitoring with the water level monitoring system; (ii) Segment joint opening monitoring with the crack meter; and (iii) Structural crack monitoring.

The joint opening monitoring data for 224 days (from April 27, 2010 to December 6, 2010) were obtained and shown in Fig. 19(b). It is obviously seen that the measured data is very stable and do not change much. The maximum joint opening is -0.183mm. According to the corporate code of the power tunnel structural safety monitoring system (Shi *et al.* 2005), the warning and

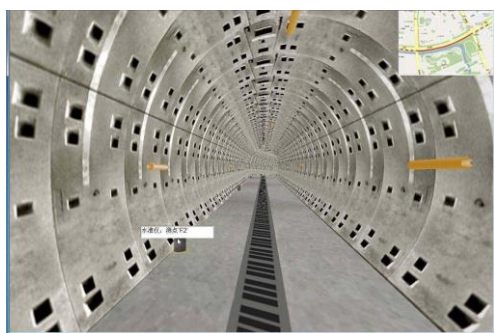
dangerous threshold values of segment joint opening are 1 mm and 2.5 mm, respectively. The maximum joint opening is much less than the warning value and the power tunnel was in a safe state.

2.6 Dams

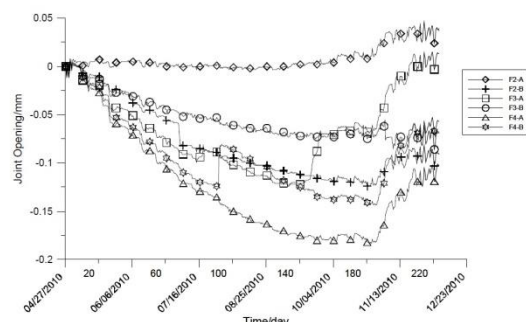
Dam is quite different from other civil infrastructure in that it is dangerous to people who live at downstream areas once collapsed. Therefore, the dams are mandated for continual surveillance including the keeping and interpretation of operational data. The SHM is equivalent to surveillance in the dam engineering community (Zhang *et al.* 2008). Not only static structural effects, but also dynamic external influences are monitored, especially, dynamic response monitoring of dams plays an important part for two reasons (Zhao and Xu 2010). First, earthquakes pose a serious threat to the safety of dams and every opportunity is taken to improve understanding of seismic dam performance. Second, estimates of dam dynamic characteristics obtained from ambient monitoring or deliberate forced vibration provide a way to track the structural characteristics as indicators of structural health, which can be seen clearly in the Three Gorges Dam.

The Three Gorges Dam is a hydroelectric dam that spans the Yangtze River in Yichang, Hubei province as shown in Fig. 20. It is the world's largest power station in terms of installed capacity 22,500 MW (Li 2000) and the largest operating hydroelectric facility in terms of annual energy generation, generating 83.7 TWh in 2013 and 98.8 TWh in 2014. The dam is a concrete gravity dam, in which the overflow dam is in the middle, two power plants are on both sides. The total length of dam axis is 2309.47m with the crest elevation of 185 m and the maximum dam height of 181 m. The normal reservoir storage water level is 175 m, the total reservoir storage capacity is 39.3 billion m³, of which flood control reservoir storage capacity is 22.15 billion m³. The Three Gorges Project has the comprehensive functions of flood control, power generation, navigation, etc.

To monitor the super-large dam both in-construction and service, around 11,280 monitoring sensors and instrument were installed (Yan and Li 2002). These sensors were equipped to measure the static structural effect, such as, the relative or absolute displacements, horizontal crest displacements, strains (for concrete dams) with a temperature correction, uplift pressures quantifying loads, seepage rates, water level, structural temperature and meteorological conditions.



(a) Shield power tunnel



(b) Measured differential settlement

Fig. 19 SHM system of the Shanghai Expo Power Tunnel (Xie and Feng 2012)

Table 6 List of dams installed with SHM in mainland China

No	Project Name	Location / Date	Capacity(KW)		Sensors (Amount)	SHM Experience
			Length	Height(m)		
1	Three Gorges Dam	Hubei 1994- 2006	18200,000	2309.47×185	StrainS(5072);PiezM(1470);DPL&IPL(175);EW(351);DG(2070);ExtM(117);DiasM(97);HL(221);IB(124);InclM(25);SG(36);	Installation of the monitoring sensors and concrete pouring should be simultaneous.
2	Baishan Dam	Jilin 1975- 1984	1800,000	676.5×149.5	DPL;IPL;BBM;DispS;HL;LLS	Safety monitoring automation system can improve the observation precision.
3	Ertan Dam	Sichuan 1991	3300,000	774.69×240	DPL;IPL;EW;ExtM;HL;TiltM;InclM;MPE;JM;PiezM;HT;MW;TempS;SS	Independent and reliable power supply is needed.
4	Fengman Dam	Jilin 1937	1002,500	1080×91.7	ExtM;HL;MPE;PiezM;HT;TempS;PT;LAS	All automation equipment needs a regular and comprehensive inspection and maintenance.
5	Gongboxia Dam	Qinghai 2000-2006	1500,000	429×132.2	TiltM(41);II(1476);DispS(12);JM(53);DPL+IPL(7);HL(24);MPE(4);MW(6);EW(9);PiezM(49)	Manual monitoring combined with automatic monitoring can make the data more scientific.
6	Huanren Dam	Liaoning 1958-1975	800,000	577.05×122.10	HDCN;PLCN;DispS;SG;JM(110);StraInS(6);ZSSM(19);SRM(30);PiezM(18);MW(3);PT(10);Acc(6);PSM(20);RB	For the choose of monitoring section, the position with complicated structure and geology should be considered firstly.
7	Liuxihe Dam	Guangdong 1956	42,000	255.5×78	PLC;JM;OT;MC;TempS;EL	More monitoring points are needed.
8	Xinanjiang Dam	Zhejiang 1957	662,500	466.5×105	EW(22);PLC(28);MPE(9);RT(34);DiasM;ODOM	Monitoring system need to achieve long-term stability
9	Longtan HydroPower Station	Guangxi 2001-2009	6300,000	830.5×216.5	DispS(114);RBE(231);TD(187);RT(34);JM(2);IB(28);Flu(53);RG	Burying of the SHM instrument should be anterior to the construction.
10	Qingtongxia Dam	Ningxia 1958-1960	272,800	678.3×42.7	PLC(13);IJM(3);EW(39)	Accuracy of the automatic monitoring system is better than optical measurement.
11	Yunfeng Dam	Jilin 1959-1967	400,000	828×113.75	PT(101);VTM (5);MPT(14);RT;HL(7)	Automatic monitoring equipment should be strengthened.
12	Yanguoxia Dam	Gansu 1958-1963	471,200	321×57.2	PLC(4);EW(22);HL(6);PiezM(4);RT;SS	
13	Xiaowan Dam	Yunnan 2002-2011	4200,000	892.786×292	JM;GPS;MPE;PiezM;StrainS;PT;Acc;SprialSTiltM;TotalS;HL	Monitoring sites of dam and diversion system can be directly connected to the power station.
14	Gongju Dam	Sichuan 1966	770,000	402×85	JM;PLC;StrainS;PiezM	Dam crest horizon displacement and dam heel stress show in yearly cycle changes
15	Gezhou Dam	Hubei 1971	2715,000	2606.5×47	EW;JM;StrainS;PiezM;IC;TempS;PT;EPC	The sheer capacity in the geological shear zone is low.
16	Wohu Mountain Reservoir Dam	Shandong 1958	-	985×37	PiezM(28);StandP(12)	Field bus technology have more advantages on implemented and economy
17	Sanmenxia Dam	Henan 1957	400,000	713.2×106	TiltM ;StandP;PLC;PiezM	Existing safety monitoring program is not perfect and monitoring data is too few.
18	Shangyoujiang Dam	Jiangxi 1955	60,000	153×67.5	JM;VC;PT;TempS;StrainS;RT;TW;MC;Level;Stopwatch	Observation facilities need to be updated
19	Taiping Bay Dam	Liaoning 1978	190,000	1185×31.5	PI(7);TW(6);PT(115);LLT(4);FM(84);LQM(4)	Bus communication is adopted.
20	Xiaolangdi Dam	Henan 1994- 2001	1800,000	1667×154	TempS;TiltM;SG;IJM;GPS;TotalS;PiezM;MicG;EPM;StaP;SRM;CSM;ZSSM;MPE	Fault instrument should be repaired and improved as soon as possible.

21	Liujiaxia Dam	Gansu 1958	1350,000 840×147	TiltM;StaP; PiezM; TempS; SRM; JM; DPL; Tri-PLC; SOH;	Measured value of PLC is not stable in humid environment.
22	Longyaxia Dam	Qinghai 1976	1280,000 1226×178	Bi-PLC(36);PI(6);MDM(5); EAI(318);SEAI(490);PT(217);JM(5); FAMI	Adopt stable distributed monitoring system
23	Ruzhadu Dam	Yunnan 2012	5850,000 630.06×261.5	-	Measures for anti-thunder.
24	Panjiakou Dam	Hebei 1975	430,000 1039.11×107.5	EW(96);ODOM(3);HL(25);TDM(4) Set dehumidifier and heating device to solve :PLC(22);TiltM(4);JM(3);DRM(391); moisture problem. PiezM(41);UF(2);TempS(25);TBRG(1);Flu(2)TAcc(3)	

Abbreviations: BBM - bimetal bench mark; Bi-PLC -- Bidirectional plumb line coordinator; CSM - concrete strain meter; DG - deformation gauge; DiasM - diastimeter; DPL - direct plumb line; EAI - Embedded automated instrument; EDM - electromagnetic distance measurement; EL - electronic level; EPC - earth pressure cell; EPM - earth pressure meter; EW - extended wire; ExtM – Extensometer; FAMI - fault activity measurement instrument; Flu --Fluviograph; FM - flow meter; HDCN - Horizontal displacement control network; HL - hydrostatic leveling; IB -inclinometer borehole; IC - inclinometer casing; II - interior instrument; IJM - interface joint meter; InclM- inclinometer; IPL - inverted plumb line; JM - joint meter; LAS - laser alignment system; LDMS - Laser displacement measurement system; LLS - liquid level sensor; LLT - liquid level transmitter; LQM - Leakage meter; MCUP - Measuring cup; MC - micrometer calipers; MDM - multi-point displacement meter; MicG - Microbarograph; MPE - multiple position extensometer; MPT-micro pulse transducer; MW - measuring weir; ODOM -odometer; OT - optical theodolite; PI - plumb instrument; PiezM - piezometer; PLCN - Precise leveling control network; PLC-plumb line coordinator; PSM-plate strain meter; PT - pressure transmitter; RBE - rock bolt extensometer; RG - Rain gauge; RT - Resistance thermometer; SEAI - Semi embedded automated instrument; SG - settlement gauge; SOH - Seepage observation hole; SOI - Seepage observation instrument; SprialS - spiral sensor; SRM - steel rebar meter; SS - Stevenson Screen; TDC - three dimensional coordinator; TiltM - Tiltmeter; Tri-PLC -- triaxial plumb line coordinator; TW - triangular weir; UF - ultrasonic flowmeter; VC - vernier caliper; VTM-Volumetric meter; ZSSM - zero stress-strain meter;

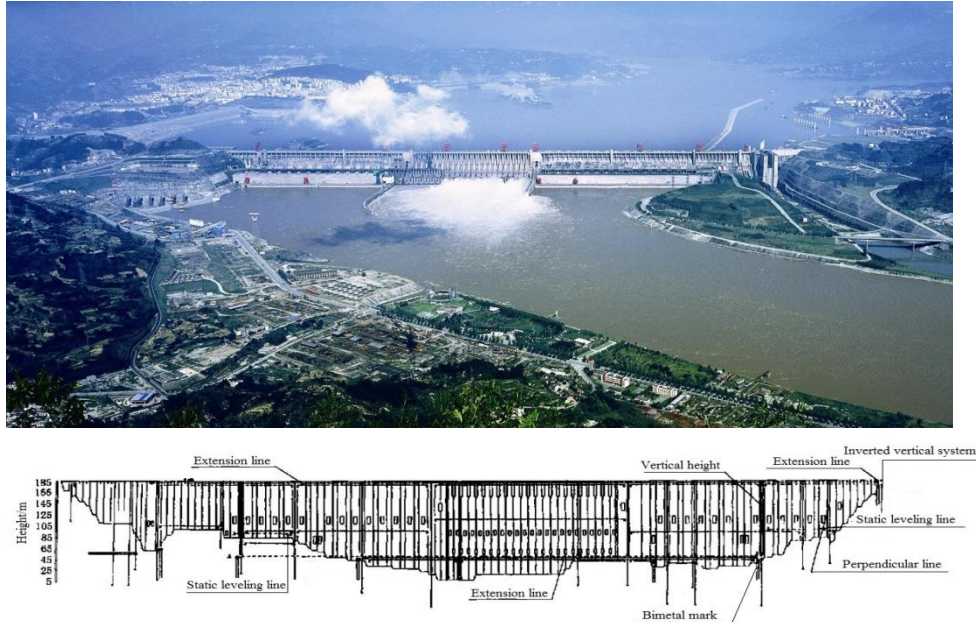
3. Challenging issues and future trends of SHM

Successful implementation of SHM systems on various civil infrastructures in mainland China has been comprehensively surveyed. Based on the above statistics and case studies, several recent tendencies in the SHM practice for large and complex civil infrastructures are worth mentioning:

(1) The designs of SHM system have become more and more with a required part of the infrastructure design and being integrated into the structural design stage. This process of integrating SHM systems reflects the owners' important concerns of structural safety in the long term. Furthermore, each SHM system is specifically designed and user tailored for certain monitoring purposes. For example, wind is an indispensable monitoring item for large space sport avenues while water leakage is an essential part of tunnel monitoring.

(2) The implementation of SHM system is performed with the civil infrastructure construction progress synchronously. For example, fiber optic sensors were installed in both the Dalian Gymnasium and Stadium during their construction phase and thus monitored during the construction progress.

(3) The SHM has extended its domain to include the in-construction monitoring besides the in-service real-time monitoring, which is a natural consequence since the SHM has been incorporated into the structural design and construction phase. The Guangzhou New TV Tower is such a typical example although functions with the in-construction monitoring and in-service real-time monitoring differs in certain aspects.



(a) Bird view of the Three Gorges Dam and (b) Crest displacement monitoring arrangement

Fig. 20 SHM system of the Three Gorges Dam (Yan and Li 2002)

In light of the significant advances and interesting trends of SHM applications in civil engineering structures, the SHM is far from mature and there are still many challenges to be resolved (Brownjohn 2007), among which three critical issues (3E issues) are discussed as follows:

(1) Efficient sensor placement.

Many sensors are needed to capture structural dynamic responses in various forms, i.e., the acceleration, velocity, displacement, temperature, and ambient wind load etc. These sensors are expected to install at critical positions or critical structural members to monitor possible changes of structural properties in the local sense as well as to gather information for damage identification algorithms to judge the damage occurrence, location and possibly damage degree in the global sense (Li *et al.* 2012). If inappropriately installed, the sensors cannot provide sufficient information for the subsequent damage identification and SHM (Yi *et al.* 2011). On the other hand, there is a tendency to over instrument a structure since it will be more difficult to add more sensors of post-construction as pointed out by Brownjohn (2007). Over-instrumentation will result in huge data storage and the overloaded data cannot, in most cases, be timely processed to extract meaningful features on current structural status. However, over-instrumentation may also compensate for the inability of effective damage identification method to some degree in practice. While standards provide guidance for practices of installing and using the SHM systems, the actual sensors, equipment and monitoring system used for the SHM are important in deciding the actual SHM performance levels. A vital portion of knowing how to select the optimal sensors and monitoring systems, however, is heavily reliant on the experience of the user. Through the knowledge of existing setups as well as the user's own experiences, the user can minimize problems (e.g., the costs, installation, time delay, etc.), and maximize performance (e.g., the

maximum sensitivity, cost vs performance ratio, safety, etc.) depending on specific features of the structure in question.

(2) Effective damage identification.

One challenge is the absence of effective damage identification methods in the field practice. Although many civil structures have been extensively deployed with sensors, one essential step is to correctly interpret the data from various types of sensors to reach critical decisions regarding the load capacity, system reliability and durability, i.e., the health condition of the structure. How to combine those single measurements to get a whole picture of structural health is still an unsolved issue. As commented in the Introduction, a successful damage identification in the structural level but not member level is still rare (Maeck *et al.* 2001, Roeck *et al.* 2003). One possible solution maybe substructure level damage identification adapted to the characteristics of each part, for instance, the cable and deck together for the suspension bridge. Furthermore, the damage is basically a local phenomenon, the damage detection methods based on the direct identification of local physical parameters, for instance, the stiffness and damping coefficients (Zhan *et al.* 2014, Nayeri *et al.* 2008), statistical properties of structural responses (Li *et al.* 2013, Alamdari *et al.* 2015) and wave propagation based methods may be feasible (Mohammadtaghi *et al.* 2015).

(3) Eliminating environmental and operational influences.

From the above survey, one can obviously observe that most SHM systems are struggling with removing ambient influences (Kullaa 2004, Manson 2002), especially temperature, which is the main factor to affect the bridge deck deflection and the joint connection (Bolton *et al.* 2001). Temperature affects the Young's modulus of many materials, thus the stiffness distribution of a structure is changed with temperature (Alampalli 2000, Moaveni *et al.* 2009). Moreover, thermal expansion and contraction render joint connections and boundary conditions of a structure varied. Although these effects can be partially mitigated in certain short term applications, it is difficult to filter out during a long term monitoring (Deraemaeker *et al.* 2008, Liu and DeWolf 2007, Ni *et al.* 2005). One example is that during the cable stretching monitoring of Dalian Gymnasium, the temperature influence can be compensated by using the FBG temperature sensors (Jia *et al.* 2011), but for the long-term monitoring after construction, the temperature poses as an obstacle in extracting the useful information from the mixed signals. Other environmental factors, such as the humidity, rain, chemicals like chloride and salt, are also concerned for damage identification and the life-cycle performance of a structure (Sohn 2007). Furthermore, operational influences including the wind, ambient loading conditions, operational speed and mass loading also cause time-varying changes of a structure (Ou and Li 2010).

These time-varying environmental and operational changes can often mask subtler structural changes caused by the damage since the dynamic features of a structure are also sensitive to the variations in the ambient temperature and operational conditions as well. To eliminate these environmental and operational influences, data normalization methods such as the factor analysis (Yan *et al.* 2005), statistical means (Sohn, 2007), co-integration, outlier analysis and principal component analysis (Cross *et al.* 2012) and recent state-space reconstruction (Figueiredo *et al.* 2010) may be employed. In fact, such non-stationary changes in the structural state requires a corresponding time-varying structural model based on the consistent load–effect relationship

Acknowledgements

The authors appreciate the significant SHM works of the researchers and engineers listed in the

paper and apologize to those not cited due to paper length limitation. Moreover, this survey was jointly supported by the National Natural Science Foundation of China (Grant No.51121005, 51578107) and 973 Project (2015CB057704).

References

- Aktan, A.E. (2009), "Characterizing highway bridges", *Proceedings of the SPIE : Smart Structures and Materials*, CA, USA, March.
- Alamdari, M.M., Samali, B. and Li, J. (2015), "Damage localization based on symbolic time series analysis", *Struct. Control Health Monit.*, **22**(2), 374-393.
- Alampalli, S. (2000), "Effects of testing, analysis, damage and environment on modal parameters", *Mech. Syst. Signal. Pr.*, **14**(1), 63-74.
- Alvandia, A. and Cremona, C. (2006), "Assessment of vibration-based damage identification techniques", *J. Sound. Vib.*, **292**(1-2), 179-202.
- Bhalla, S., Yang, Y.W., Zhao, J. and Soh, C.K. (2005), "Structural health monitoring of underground facilities—Technological issues and challenges", *Tunn. Undergr. Sp. Tech.*, **20**(5), 487-500.
- Bolton, R., Stubbs, N., Park, S., Sikorsky, C. and Choi, S. (2001), "Documentation of changes in modal properties of a concrete box-girder bridge due to environmental and internal conditions", *Comput-Aided. Civ. Inf.*, **16**(1), 42-57.
- Brownjohn, J.M. (2007), "Structural health monitoring of civil infrastructure", *Philos. T. R. Soc. A.*, **365**(1851), 589-622.
- Cross, E., Manson, G., Worden, K. and Pierce, S. (2012), "Features for damage detection with insensitivity to environmental and operational variations, proceedings of the royal society a: mathematical", *Phys. Eng. Sci.*, **468**(2148), 4098-4122.
- Deraemaeker, A., Reynders, E., De Roeck, G. and Kullaa, J. (2008), "Vibration based structural health monitoring using output-only measurements under changing environment", *Mech. Syst. Signal. Pr.*, **22**(1), 34-56.
- Doebling, S.W., Farrar, C.R., Prime, M.B., et al. (1996), *Damage identification and health monitoring of structural and mechanical systems from changes in their vibration characteristics: a literature review*, Los Alamos National Laboratory Report, LA,NM.
- Erturk, A. and Inman, D.J. (2011), *Piezoelectric Energy Harvesting*, Wiley.
- Fan, W. and Qiao, P.Z. (2011), "Vibration-based Damage Identification Methods: A Review and Comparative Study", *Struct. Health. Monit.*, **10**(1), 83-111.
- Farrar, C.R. and Worden, K. (2013), *Structural Health Monitoring - A Machine Learning Perspective*, John Wiley & Sons Ltd, Chichester, UK.
- Figueiredo, E., Todd, M., Farrar, C. and Flynn, E. (2010), "Autoregressive modeling with state-space embedding vectors for damage detection under operational variability", *Int. J. Eng. Sci.*, **48**(10), 822-834.
- Hu, J., Li, H., Yang H.Z., Zhang Q.L.(2014), "Integrated design and application structural health monitoring software system of Shanghai Tower", *J. Tongji Univ. (Natural Science)*, **42**(3), 460-467.
- Huang, F.L., He, X.H., Chen, Z.Q. and Zeng, C.H. (2004), "Structural safety monitoring for Nanjing Yangtze River Bridge", *J. Cent. South. Univ. Technol.*, **11**(3), 332-335.
- Jia, Z., Ren, L., Li, D. and Li, H. (2011), "Cable stretching construction monitoring based on FBG sensor", *Proceedings- SPIE the International Society for Optical Engineering*. San Diego, CA.
- Kullaa, J. (2004), "Structural health monitoring under variable environmental or operational conditions", *Proceedings of the 2nd European Workshop on Structural Health Monitoring*, Munich, Germany.
- Li, A.Q., Ding, Y.L., Deng, Y., Yao B., Yang, J. and Zhou, J.H. (2010), "Technology and application of structural health condition assessment for Sutong Bridge (2): damage alarming of main girder", *J. Dis. Prev. Mitig. Engr.*, **30**(3), 330-335.

- Li, D.S., Li, H.N. and Fritzen, C.P. (2012), "Load dependent sensor placement method: theory and experimental validation", *Mech. Syst. Signal. Pr.*, **31**, 217-227.
- Li, D.S., Li, H.N., Ren, L. and Song, G. (2006), "Strain transferring analysis of fiber Bragg grating sensors", *Opt. Eng.*, **45**(2), 4402.
- Li, H. N., Li, D. S. and Song, G. B. (2004), "Recent applications of fiber optic sensors to health monitoring in civil engineering", *Eng. Struct.*, **26**(11), 1647-1657.
- Li, H.N., Yi, T.H., Ren, L., Li, D.S. and Huo L.S.(2014), "Reviews on innovations and applications in structural health monitoring for infrastructures", *Struct. Monit. Maint.*, **1**(1),1-45.
- Li, H.N., Yi, T.H., Yi, X.D. and Wang, G.X. (2007), "Measurement and analysis of wind-induced response of tall building based on GPS technology", *Adv. Struct. Eng.*, **10**(1), 83-93.
- Li, N. (2000), "Brief talk of the action of dam security monitoring system on construction and operation of Three Gorges Dam", *Exp. Tech. Manag.*, **17**(4), 80-84.
- Li, R., Mita, A. and Zhou, J. (2013), "Symbolization-based differential evolution strategy for identification of structural parameters", *Struct. Control Health Monit.*, **20**(10), 1255-1270.
- Liu, C. and DeWolf, J. (2007), "Effect of temperature on modal variability of a curved concrete bridge under ambient loads", *J. Struct. Eng. - ASCE.*, **133**(12), 1742-1751.
- Liu, S.C., Zhang, D.L., Huang, J. and Zhang, C.P. (2011), "Research and design on structural health monitoring System for Large-scale Shield Tunnel", *Chinese Journal of Underground Space and Engineering*, **7**(4), 741-748.
- Lu, W. (2010), *The structural health monitoring system of large span space structure based on field bus*, Ph.D. Dissertation, Harbin Institute of Technology, Harbin.
- Lynch, J.P. (2007), "An overview of wireless structural health Monitoring for Civil Structures", *Philos. T. Roy. Soc. A.*, **365**(1851), 345-372.
- Maeck, J., Peeters, B. and De Roeck, G. (2001), "Damage identification on the Z24 bridge using vibration monitoring analysis", *Smart Mater. Struct.*, **10**(3), 512-517.
- Manson, G. (2002), "Identifying damage sensitive, environment insensitive features for damage detection", *Proceedings of the 3rd International Conference on Identification in Engineering Systems*, University of Wales Swansea, UK.
- Messina, A., Williams, E.J. and Contursi, T. (1998), "Structural damage detection by a sensitivity and statistical-based method", *J. Sound. Vib.*, **216**(5), 791-808.
- Min, F.L., Zhu, W., Lin, C. and Guo, X.J. (2015), "Opening the excavation chamber of the large-diameter size slurry shield: A case study in Nanjing Yangtze River Tunnel in China", *Tunn. Undergr. Sp. Tech.*, **46**(2), 18-27.
- Moaveni, B., He, X.F., Conte, J.P., Fraser, M.S. and Elgamal, A. (2009), "Uncertainty Analysis of Voigt Bridge Modal Parameters Due to Changing Environmental Conditions", *Proceedings of the IMAC-XXVII*, Florida, USA, February.
- Mohammadtaghi, R., Mahdi, E. and Maria, I.T. (2015), "Wave dispersion in high-rise buildings due to soil-structure interaction", *Earthq. Eng. Struct. D.*, **44**(2), 317-323.
- Nayeri, R.D., Masri, S.F., Ghanem, R.G. and Nigbor, R.L. (2008), "A novel approach for the structural identification and monitoring of a full-scale 17-story building based on ambient vibration measurements", *Smart. Mater. Struct.*, **17**(2), 1-19.
- Ni, Y.Q., Hua, X.G., Fan, K.Q. and Ko, J.M. (2005), "Correlating modal properties with temperature using long-term monitoring data and support vector machine technique", *Eng. Struct.*, **27**(12), 1762-1773.
- Ni, Y.Q., Xia, Y., Liao, W.Y. and Ko, J.M. (2009), "Technology innovation in developing the structural health monitoring system for Guangzhou New TV Tower", *Struct. Control Health.*, **16**(1), 73-98.
- Ou, J.P. (2003), "Some recent advances of intelligent health monitoring systems for civil infrastructures in mainland China", *Proceeding of the 1st International Conference on Structural Health Monitoring and Intelligent Infrastructure*, Tokyo, Japan.
- Ou, J.P. and Li, H. (2010), "Structural Health Monitoring in mainland China: Review and Future Trends", *Struct. Health. Monit.*, **9**(3), 219-231.
- Ou, J.P., Xiao, Y.Q., Huang, H.J., Hai, Z.D., Zhang, T. and Li, W.X. (2001), "Real time safety monitoring

- system for offshore platform structures”, *Ocean Eng.*, **19**(2), 1-6.
- Pandey, A.K., Biswas, M. and Samman, M.M. (1991), “Damage detection from changes in curvature mode shapes”, *J. Sound. Vib.*, **145**(2), 321-332.
- Peeters, B., Maeck, J. and Roeck, G.D. (2001), “Vibration-based damage detection in civil engineering: excitation sources and temperature effects”, *Smart. Mater. Struct.*, **10**(3), 518-527.
- Roeck, G.D. (2003), “The state-of-the-art of damage detection by vibration monitoring: the SIMCES experience”, *J. Struct. Control.*, **10**(2), 127-134.
- Salawu, O.S. and Williams, C. (1995), “A review of full-scale dynamic testing of bridge structures”, *Eng. Struct.*, **17**(2), 113-121.
- Shi, B., Xu, X. J., Wang, D., Wang, T., Zhang, D., Ding, Y., Xu, H.Z. and Cui, H.L. (2005), “Study on BOTDR-based distributed optical fiber strain measurement for tunnel health diagnosis”, *Chinese J. Rock Mech. Eng.*, **24**(15), 2622-2628.
- Sohn, H. (2007), “Effects of environmental and operational variability on structural health monitoring”, *Philos. T. Roy. Soc. A.*, **365**(1851), 539-560.
- Sohn, H., Dzwonczyk, M., Straser, E., Kiremidjian, A., Law, K. and Meng, T. (1999), “An experimental study of temperature effect on modal parameters of the Alamos Canyon Bridge”, *Earthq. Eng. Struct. D.*, **28**(8), 879-897.
- Sohn, H., Farrar, C.R., Hemez, and F.M., et al. (2004), *A review of structural health monitoring literature: 1996-2001*, Los Alamos National Laboratory Report, LA, NM.
- Su, J.Z., Xia, Y., Chen, L., Zhao, X., Zhang, Q.L., Xu, Y.L., Ding, J.M., Xiong, H.B., Ma, R.J., Lv, X.L. and Chen, A. R. (2013), “Long-term structural performance monitoring system for the Shanghai Tower”, *J. Civil. Struct. Health. Monit.*, **3**(1), 49-61.
- Vanlanduit, S., Parloo, E., Cauberghe, B., Guillaume, P. and Verboven, P. (2005), “A robust singular value decomposition for damage detection under changing operating conditions and structural uncertainties”, *J. Sound. Vib.*, **284**(3-5), 1033-1050.
- Visser, W. (2004), “Ship collision and capacity of brace members of fixed steel offshore platforms”, *HSE books*, research report 220, 1-10.
- Wang, Y.L., Yue, Q.J., Guo, F.W., Bi, X.J., Shi, Z.M., Qu, Y. (2012), “Performance evaluation of a new ice-resistant jacket platform based on field monitoring”, *Cold. Reg. Sci. Technol.*, **71**, 44-53.
- Worden, K., Farrer, C. R., Manson, G. and Park, G. (2007), “The fundamental axioms of structural health monitoring”, *P. Roy. Soc. A-Math. Phys.*, **463**(2082), 1639-1664.
- Xie, X.Y. and Feng, L. (2012), “Real-time health monitoring system for power tunnel”, *Proceeding of the Geo-Institute’s 2012 Annual Congress*, Oakland, CA.
- Yan, A.M., Kerschen, G., Boe, P.D. and Golinval, J.C. (2005), “Structural damaged diagnosis under varying environmental conditions - part I: a linear analysis”, *Mech. Syst. Signal. Pr.*, **19**(4), 847-864.
- Yan, J.G. and Li, S.P. (2002), “Design optimization of Three Gorges Dam deformation monitoring”, *Yangtze River*, **33**(6), 36-38.
- Yi, T.H., Li, H.N. and Gu, M. (2011), “Optimal sensor placement for structural health monitoring based on multiple optimization strategies”, *Struct. Des. Tall. Spec.*, **20**(7), 881-900.
- Yi, T.H. and Li, H.N. (2012a), “Methodology developments in sensor placement for health monitoring of civil infrastructures”, *Int. J. Distrib. Sens. N.*, Article ID 612726, 1-11.
- Zhan, C., Li, D.S. and Li, H.N. (2014), “A local damage detection approach based on restoring force method”, *J. Sound Vib.*, **333**(20), 4942-4959.
- Zhang, J.P., Li, L. and Lu, Z.C. (2008), “Review and prospect of dam safety monitoring”, *J. China Inst. Water Resour. Hydropower Res.*, **6**(4), 316-322.
- Zhao, Z.R. and Xu, R. (2010), “Advance and prospect of monitoring technology for dam safety”, *Hydropower Automation and dam monitoring*, **34**(5), 52-57.